iScience

CellPress
OPEN ACCESS

Article

Distinct pathways for export of silencing RNA in *Caenorhabditis elegans* systemic RNAi

RNAi target tissues	germ cells		intestine
dsRNA introduction	feeding	pseudocoelomic injection	feeding
Wild type	sensitive	sensitive	sensitive
dsRNA export mutant (*rexd-1; tbc-3; sid-5*)	resistant	sensitive	sensitive
dsRNA import mutant (*sid-1, rsd-3* etc.)	resistant	resistant	resistant

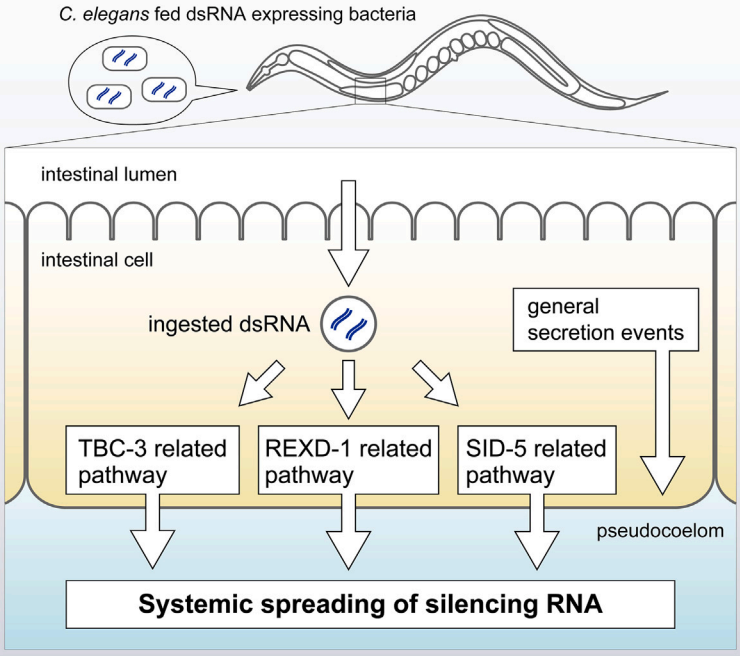

Keita Yoshida, Yuji Suehiro, Katsufumi Dejima, Sawako Yoshina, Shohei Mitani

mitani.shohei@twmu.ac.jp

Highlights

REXD-1 and TBC-3 were identified as novel systemic RNAi regulators

REXD-1, TBC-3, and SID-5 act in parallel pathways to regulate systemic RNAi

The *rexd-1; tbc-3; sid-5* triple mutant was defective in the dsRNA export from cells

The RabGAP TBC-3 acts in the endosome-to-Golgi trafficking pathway

Yoshida et al., iScience *26*, 108067
October 20, 2023
https://doi.org/10.1016/j.isci.2023.108067

iScience

CellPress
OPEN ACCESS

Article

Distinct pathways for export of silencing RNA in *Caenorhabditis elegans* systemic RNAi

Keita Yoshida,[1] Yuji Suehiro,[1] Katsufumi Dejima,[1] Sawako Yoshina,[1] and Shohei Mitani[1,2,*]

SUMMARY

Dietary supplied double-stranded RNA (dsRNA) can trigger RNA interference (RNAi) systemically in some animals, including the nematode *Caenorhabditis elegans*. Although this phenomenon has been utilized as a major tool for gene silencing in *C. elegans*, how cells spread the silencing RNA throughout the organism is largely unknown. Here, we identify two novel systemic RNAi-related factors, REXD-1 and TBC-3, and show that these two factors together with SID-5 act redundantly to promote systemic spreading of dsRNA. Animals that are defective in all REXD-1, TBC-3, and SID-5 functions show strong deficiency in export of dsRNA from intestinal cells, whereas cellular uptake and processing of dsRNA and general secretion events other than dsRNA secretion are still functional in the triple mutant animals. Our findings reveal pathways that specifically regulate the export of dsRNA in parallel, implying the importance of spreading RNA molecules for intercellular communication in organisms.

INTRODUCTION

RNA interference (RNAi) is a gene silencing mechanism triggered by double-stranded RNA (dsRNA).[1] In some animals, including the nematode *Caenorhabditis elegans*, the RNAi response can be spread throughout the body from a tissue where dsRNA is initially introduced or expressed,[1,2] a phenomenon referred to as systemic RNAi. In *C. elegans*, systemic RNAi can be induced upon soaking animals in a solution containing dsRNA or feeding on bacteria expressing dsRNA (feeding RNAi).[3,4] This property of RNAi revolutionized genetic analysis in *C. elegans*, e.g., enabling high-throughput, genome-wide RNAi screens.[5–8]

In feeding RNAi, dsRNA must be first taken up by intestinal cells from the intestinal lumen, exported from intestinal cells to the pseudocoelom, the body cavity in *C. elegans*, and then imported into the cytosol of other cells where processing of dsRNA occurs to generate small interfering RNA.[9] Forward genetic screens identified genes, each of which is involved in a respective step of feeding RNAi.[2,10] The dsRNA importer systemic RNAi defective-1 (SID-1) is required for the import of dsRNA into the cytosol but dispensable for the export of dsRNA.[11,12] SID-2 is a transmembrane protein localized to the apical membrane of intestinal cells and required for dsRNA uptake from the intestinal lumen.[13,14] SID-3 and NCK-1/SID-4, homologs of ACK1 kinase and its interactor NCK protein, respectively,[15,16] and an ENTH domain protein RSD-3[10,17] have been shown to be involved in the import of silencing signals from the pseudocoelom. Regulators of the endocytic pathway that mediate dsRNA uptake into *Drosophila* S2 cells are also suggested to be involved in cell entry of dsRNA in *C. elegans*.[18] SID-5 is a single-pass transmembrane protein and associates with late endosomes.[19] Expression of SID-5 in the intestine is required for RNAi silencing in the body wall muscles upon dsRNA ingestion, suggesting a possible function of SID-5 in dsRNA export out of cells.[19] However, it is also possible that SID-5 facilitates dsRNA secretion indirectly by cytosolic release of dsRNA in the intestine.[20] It is thus still unclear how cells export dsRNA, which is a crucial step for systemic RNAi.

Here, we identify and characterize novel regulators of systemic RNAi. One is a previously uncharacterized protein REXD-1 that we named, and the other is a conserved TBC domain-containing protein TBC-3. These two factors can promote RNAi silencing in a non-cell autonomous manner similar to SID-5. Triple mutant animals harboring *rexd-1*, *tbc-3*, and *sid-5* mutations show strong resistance to feeding RNAi except for genes expressed in the intestine, but they are sensitive to the injection of dsRNA into the pseudocoelom, suggesting that REXD-1, TBC-3, and SID-5 constitute distinct pathways to regulate export of dsRNA from cells. We also show that TBC-3 acts in the endosome-to-Golgi trafficking pathway to mediate dsRNA transport. Our findings reveal a specific and robust mechanism to control the export of dsRNA, suggesting the significance of spreading RNAs as signaling molecules between cells.

RESULTS

Identification and characterization of a novel systemic RNAi regulator

Membrane trafficking pathways, which are regulated by a number of specialized proteins including Rab small GTPases,[21] are considered to be important in systemic spreading of silencing RNA.[17,19] We previously tested sensitivity to feeding RNAi in various mutants of membrane

[1]Department of Physiology, Tokyo Women's Medical University School of Medicine, 8-1, Kawada-cho, Shinjuku-ku, Tokyo 162-8666, Japan
[2]Lead contact
*Correspondence: mitani.shohei@twmu.ac.jp
https://doi.org/10.1016/j.isci.2023.108067

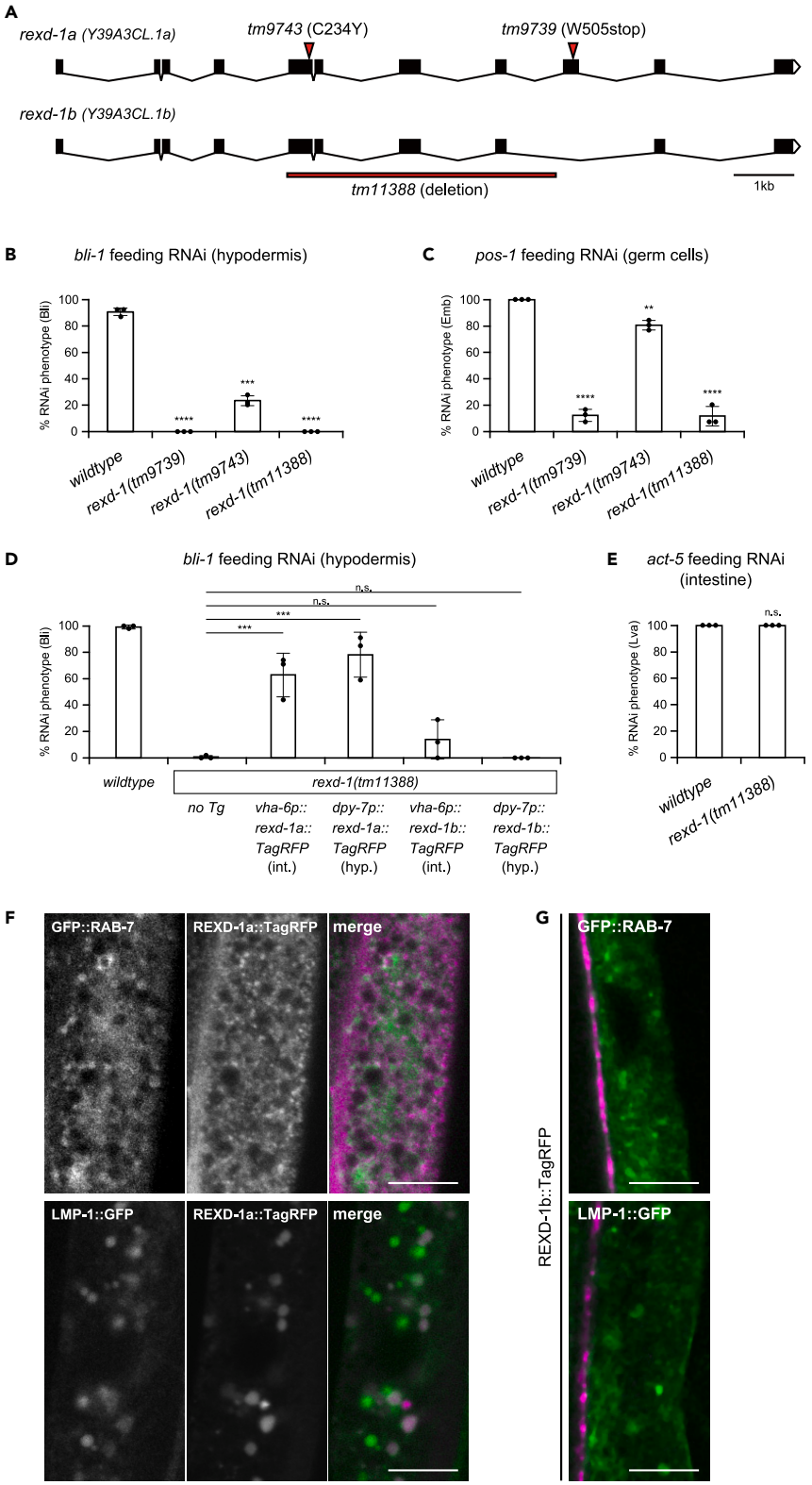
A
rexd-1a (Y39A3CL.1a)
tm9743 (C234Y)
tm9739 (W505stop)
rexd-1b (Y39A3CL.1b)
tm11388 (deletion)
1kb
B
bli-1 feeding RNAi (hypodermis)
% RNAi phenotype (Bli)
wildtype
rexd-1(tm9739)
rexd-1(tm9743)
rexd-1(tm11388)
C
pos-1 feeding RNAi (germ cells)
% RNAi phenotype (Emb)
D
bli-1 feeding RNAi (hypodermis)
n.s.
wildtype
rexd-1(tm11388)
no Tg
vha-6p::rexd-1a::TagRFP (int.)
dpy-7p::rexd-1a::TagRFP (hyp.)
vha-6p::rexd-1b::TagRFP (int.)
dpy-7p::rexd-1b::TagRFP (hyp.)
E
act-5 feeding RNAi (intestine)
% RNAi phenotype (Lva)
F
GFP::RAB-7
REXD-1a::TagRFP
merge
LMP-1::GFP
G
REXD-1b::TagRFP

Figure 1. REXD-1 is a membrane-associated protein and involved in systemic RNAi

(A) Gene structure of *rexd-1* (*Y39A3CL.1*). Mutation sites of *tm9739* and *tm9743*, which are isolated in our screen, and the deletion region of *tm11388* are indicated. Filled and open boxes indicate the coding sequence and untranslated regions, respectively.

(B) Percentage of animals that showed the blister (Bli) phenotype upon feeding RNAi against the hypodermal gene *bli-1*.

(C) Percentage of embryonic lethality of F1 progeny of animals fed bacteria expressing dsRNA against the germline-expressed gene *pos-1*.

(D) Percentage of affected (Bli) animals upon feeding RNAi against *bli-1*. *vha-6p* and *dpy-7p* drive transgene (Tg) expression in the intestine (int.) and hypodermis (hyp.), respectively.

(E) Percentage of animals that showed the larval arrest (Lva) phenotype upon feeding RNAi against the intestinal gene *act-5*.

(F and G) Confocal fluorescence images of intestinal cells in young adult animals expressing REXD-1a::TagRFP (F) or REXD-1b::TagRFP (G) in combination with GFP::RAB-7 (top) or LMP-1::GFP (bottom). For merged images, TagRFP and GFP are pseudocolored magenta and green, respectively. Images of REXD-1a::TagRFP in (F) were captured with different exposure times due to different levels of transgene expression between individuals. Scale bars, 10 μm.

(B–E) Bars represent the mean (±SEM) from three independent experiments. Genotypes of tested animals are indicated at the bottom. One-Way ANOVA, Tukey's multiple comparison test. **p < 0.01, ***p < 0.001, ****p < 0.0001, n.s. = not significant. See also Figure S1.

trafficking-related genes and found that any tested mutants for Rab family genes show no obvious defects in RNAi response.[17] Thus, it is possible that the spreading of ingested dsRNA involves redundantly acting membrane trafficking pathways that are regulated by respective Rab proteins. To understand the mechanism underlying the export of silencing RNA in systemic RNAi, we conducted a forward genetic screen. To increase the chance of isolating mutants of the secretory pathway of dsRNA, we used double mutant animals of *rab-3* and *aex-6*/*rab-27* genes, which encode Rab-GTPases regulating secretory vesicle traffic.[22] The *aex-6*(*tm2302*); *rab-3*(*tm3275*) double mutant was as sensitive to feeding RNAi (Figure S1A) as each of the single mutants, suggesting that AEX-6- and RAB-3-related pathways do not function or act with redundant pathways in the systemic spreading of dsRNA. We mutagenized the double mutant using ethyl methanesulfonate (EMS) and screened for mutants that were defective in feeding RNAi (see STAR Methods for details).

From this screen, we first identified two alleles of the gene Y39A3CL.1 encoding a previously uncharacterized protein. Y39A3CL.1 has two isoforms, Y39A3CL.1a and Y39A3CL.1b, which encode 681 amino acid (AA) and 603 AA length proteins, respectively. Of the two alleles identified, *tm9739* was a nonsense mutation that is located on exon 9, which is exclusive to Y39A3CL.1a, whereas the *tm9743* mutation substituted the isoform shared cysteine 234 with a tyrosine residue (Figure 1A). To confirm the requirement of this gene for feeding RNAi, we used a deletion allele, *tm11388* (Figure 1A). The *tm11388* mutant showed resistance to feeding dsRNA targeting the hypodermis expressing *bli-1* and germline expressing *pos-1* genes. The penetrance of RNAi resistance in *tm11388* is similar to that in *tm9739* and higher than that in *tm9743*, suggesting that loss of Y39A3CL.1 function causes deficiency in feeding RNAi (Figures 1B and 1C). We crossed *tm11388* with the *aex-6*(*tm2302*); *rab-3*(*tm3275*) double mutant and found that *aex-6* and *rab-3* mutations did not strengthen the RNAi resistance of *tm11388* (Figure S1B), suggesting no functional redundancy between these factors.

Our screen identified Y39A3CL.1 as a novel factor that is required for efficient systemic RNAi. Transcriptomics data suggest that this gene is ubiquitously expressed throughout development,[23] which was supported by data on the expression of a GFP reporter fused with the putative promoter sequence (Figure S1C). To determine which process of feeding RNAi Y39A3CL.1 is involved in, we carried out tissue-specific rescue experiments. We constructed transgenes that express the TagRFP-fusion form of Y39A3CL.1a or Y39A3CL.1b under the control of intestine (*vha-6*) or hypodermis (*dpy-7*) specific promoters and tested whether these transgenes restore *tm11388* sensitivity to feeding RNAi targeting the *bli-1* gene, which is expressed in the hypodermis. We found that both intestine- and hypodermis-specific expression of Y39A3CL.1a but not Y39A3CL.1b successfully restored sensitivity to *bli-1* feeding RNAi in the mutant (Figure 1D), suggesting that of the two isoforms, only Y39A3CL.1a is involved in systemic RNAi. This is consistent with the observation that *tm9739*, which is likely to affect only Y39A3CL.1a, showed a comparable phenotype to *tm11388*, which deleted a large portion of the gene. We could not find any homologous domain in other proteins except in nematodes. It is also suggested that Y39A3CL.1 can act in a non-cell autonomous manner in systemic RNAi, as its intestinal expression rescues hypodermal RNAi sensitivity. There are two possible functions in the intestine among feeding RNAi processes: uptake of dsRNA from the intestinal lumen to intestinal cells and exporting dsRNA from intestinal cells to the pseudocoelom. Then, we tested *tm11388* for sensitivity to feeding RNAi targeting *act-5*, which is expressed in the intestine, and found that *tm11388* animals are sensitive to *act-5* RNAi as well as wild-type animals (Figure 1E). This indicates that Y39A3CL.1 is likely to be involved in dsRNA export from intestinal cells rather than dsRNA uptake from the environment. Based on this finding, we named Y39A3CL.1 *rexd-1* (*RNAi EXporting Defective*). Hypodermis-specific expression of *rexd-1* also restored *bli-1* RNAi sensitivity in the mutant. This suggests that REXD-1 is dispensable but required for efficient export of silencing RNAs from the intestine and that REXD-1 also promotes intercellular spreading and/or uptake of dsRNA in hypodermal cells, leading to a robust RNAi response in the tissue.

Expression of TagRFP-fusion REXD-1a, which rescues RNAi deficiency, was detected as cytoplasmic foci and on the apical membrane in intestinal cells. To determine the subcellular localization of REXD-1, we expressed this transgene in strains that express GFP fusions of endomembrane organelle markers.[24–26] Cytoplasmic expression of TagRFP was partially colocalized with the late-endosome-associated GFP::RAB-7 and lysosomal protein LMP-1::GFP (Figure 1F) but less with GFP::RAB-5, GFP::RAB-11 and AMAN-2::GFP, which mark early endosomes, recycling endosomes and the Golgi, respectively (Figure S1D). Similar colocalization patterns were observed using transgenes expressed in the hypodermis (Figure S1E). In contrast, REXD-1b, which is nonfunctional in systemic RNAi, is not localized to the cytosol but only to the apical membrane of intestinal cells (Figure 1G). These observations suggest that REXD-1 is associated with endomembrane trafficking systems through its isoform-specific domain and that cytoplasmic localization of REXD-1 is required for systemic RNAi. Overall, our screen identified REXD-1 as a novel systemic RNAi regulator that is associated with endomembrane trafficking and important for efficient spreading of dsRNA during systemic RNAi.

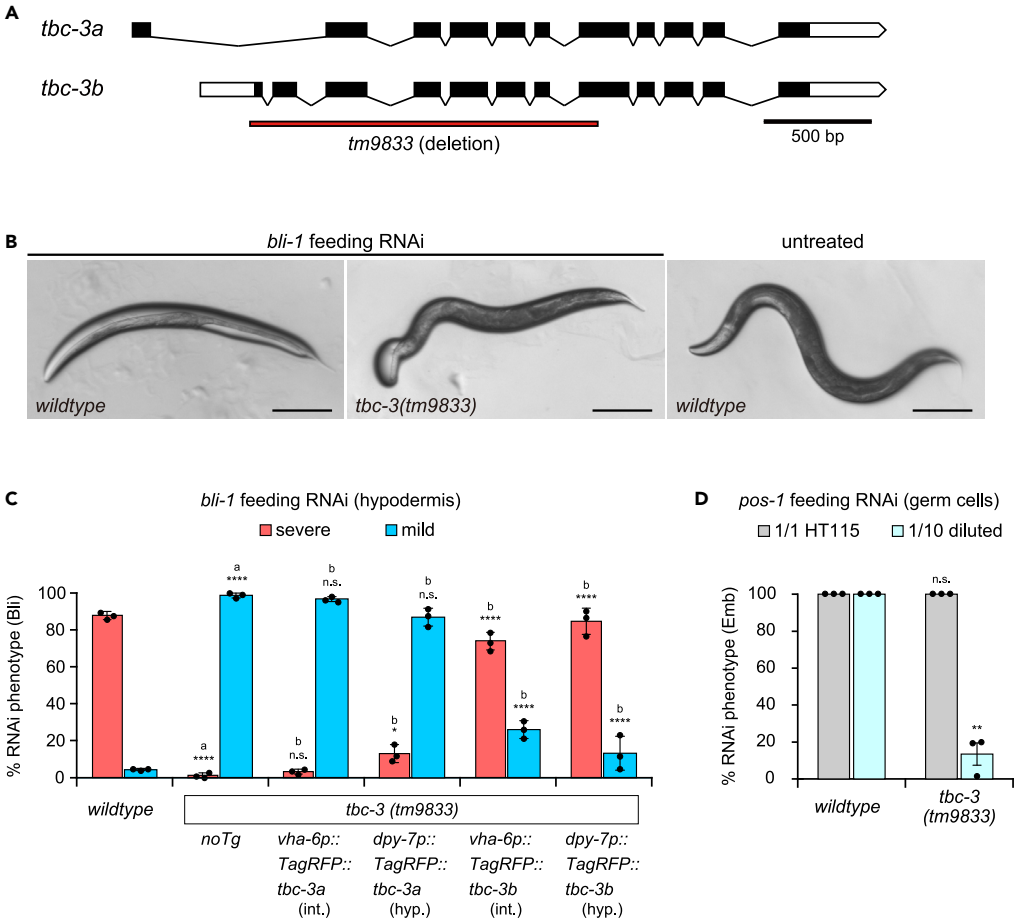

Figure 2. TBC-3 is required for efficient systemic RNAi

(A) Gene structure of *tbc-3* (*F32B6.8*). Deletion region of *tm9833* is indicated. Filled and open boxes indicate the coding sequence and untranslated regions, respectively.

(B) Representative images of adult animals fed bacteria expressing *bli-1* dsRNA or normal food (untreated). Wild-type animals showed the full-body (severe) blister phenotype (left). *tbc-3(tm9833)* mutants showed resistance to feeding RNAi and had partial (mild) blisters on their head (center). Scale bars, 200 μm.

(C) Percentage of affected animals upon feeding RNAi against the hypodermal gene *bli-1*. Bars represent the mean (±SEM) from three independent experiments. Genotypes and introduced transgenes of tested animals are indicated at the bottom. Animals showed severe and mild blister (Bli) phenotypes were separately scored. *vha-6p* and *dpy-7p* drive transgene (Tg) expression in the intestine (int.) and hypodermis (hyp.), respectively. one-way ANOVA, Tukey's multiple comparison test. a, Comparison with the wild type. b, Comparison with *tbc-3(tm9833)*. *p < 0.05, ****p < 0.0001, n.s. = not significant.

(D) Percentage of embryonic lethality of F1 progeny of animals fed bacteria expressing dsRNA against the germline-expressed gene *pos-1* in normal (1/1 HT115) and desensitized (1/10 diluted) conditions. Bars represent the mean (±SEM) from three independent experiments. Two-tailed t-test. **p < 0.01, n.s. = not significant. See also Figure S2.

RabGAP TBC-3 is involved in the transport of dsRNA

We next isolated a strain, FX30944, that harbors mutations in the *rde-11* and *tbc-3* genes from the screening (Figures S2A and S2B). Because RDE-11 is known to be involved in secondary siRNA amplification in exogenous RNAi,[27,28] we first speculated that the *rde-11* mutation is the cause of RNAi deficiency in the strain. Introduction of wild-type *rde-11*, however, partially rescued sensitivity to *bli-1* feeding RNAi (Figure S2C), suggesting that *rde-11* is not solely responsible for RNAi deficiency. Then, we focused our attention on *tbc-3*, which harbors a nonsense mutation that affects both isoforms, *tbc-3a* and *tbc-3b*. Simultaneous introduction of *rde-11* and *tbc-3* genomic DNA fragments successfully restored sensitivity to *bli-1* RNAi (Figure S2C), indicating that disruption of TBC-3 function is also responsible for deficiency in systemic RNAi.

TBC-3 is a member of the evolutionally conserved TBC domain-containing protein family, which is known to be a GTPase-activating protein (GAP) for Rab GTPases.[29,30] To characterize TBC-3 function in systemic RNAi, we generated a deletion allele, *tbc-3*(*tm9833*), using CRISPR-based genome editing (Figure 2A). When fed on bacteria expressing *bli-1* dsRNA, *tbc-3*(*tm9833*) animals showed a "mild" phenotype, appearing as partial blisters on their cuticle, whereas wild-type animals displayed "severe" whole-body blisters (Figures 2B and 2C), suggesting that loss of TBC-3 function solely causes weak deficiency in feeding RNAi. When *tbc-3*(*tm9833*) mutants were fed *pos-1* dsRNA

foods, they showed a comparable sensitivity to wild-type animals (Figure 2D), implying possible tissue specificity of TBC-3 function. However, *tbc-3*(*tm9833*) animals were resistant to *pos-1* feeding RNAi under lower-dose conditions, where dsRNA-expressing bacteria (HT115) were diluted 10 times, whereas wild-type animals were fully sensitive under the same conditions (Figure 2D). These results suggest that *tbc-3*(*tm9833*) mutants have weak and dose-dependent deficiencies in feeding RNAi targeting genes expressed in both somatic and germ cells.

To elucidate which process of systemic RNAi TBC-3 is involved in and which isoform functions in systemic RNAi, we expressed *tbc-3a* or *tbc-3b* using tissue-specific promoters in the *tbc-3*(*tm9833*) mutant and tested feeding RNAi against hypodermal *bli-1*. Intestinal expression of *tbc-3b* but not *tbc-3a* restored wild-type-like severe blisters in the *tbc-3* mutant upon feeding *bli-1* dsRNA (Figure 2C). Similarly, expression of *tbc-3b* in the hypodermis rescued RNAi sensitivity more efficiently than expression of *tbc-3a* (Figure 2C). These results suggest that of the two isoforms, *tbc-3b* mainly functions in systemic RNAi and can act in a non-cell autonomous manner during systemic spreading of dsRNA.

Next, to test the subcellular localization of TBC-3b, we expressed a TagRFP fusion form of TBC-3b in strains expressing organelle markers. TagRFP colocalized with the Golgi marker AMAN-2::GFP in intestinal cells (Figure S2D). This is consistent with previous reports that TBC-3b colocalizes with a Golgi marker in seam cells[31] and that TBC1D22B, a human ortholog of TBC-3, interacts with Golgi resident proteins.[32] In addition, we also found that TBC-3b partially colocalized with late endosome-associated RAB-7::GFP in the intestine (Figure S2D). These results suggest that the RabGAP TBC-3 is involved in the efficient spreading of silencing RNAs in systemic RNAi by regulating membrane trafficking pathways.

REXD-1, TBC-3, and SID-5 act in parallel pathways in systemic RNAi

Our previous results suggested that both REXD-1 and TBC-3 can promote systemic RNAi silencing in a non-cell autonomous manner. It has been previously reported that expression of SID-5 in the intestine is required for RNAi silencing in body wall muscles.[19] Then, we next examined whether REXD-1, TBC-3, and SID-5 act together in the transport of dsRNA between cells and generated double mutant animals of *rexd-1(tm11388)*; *tbc-3(tm9833)*, *rexd-1(tm11388)*; *sid-5(tm4328)* and *tbc-3(tm9833)*; *sid-5(tm4328)* and the *rexd-1(tm11388)*; *tbc-3(tm9833)*; *sid-5(tm4328)* triple mutant. To assay genetic interactions between *rexd-1*, *tbc-3* and *sid-5*, we observed the phenotype of each genotype upon *bli-3* feeding RNAi. When wild-type animals were fed bacteria expressing *bli-3* dsRNA, almost all of them were dead during larval stages (Figure 3; classified as the severe phenotype). Single mutant animals of *tbc-3(tm9833)* and *sid-5(tm4328)* showed the severe phenotype as did wild-type animals, whereas a small number of *rexd-1(tm11388)* mutants developed into gravid adults with blistered cuticles (classified as the mild phenotype), indicating that the solo functions of REXD-1, TBC-3 and SID-5 are dispensable for spreading ingested dsRNA (Figure 3). In contrast, double mutants of *rexd-1(tm11388)*; *tbc-3(tm9833)*, *rexd-1(tm11388)*; *sid-5(tm4328)* and *tbc-3(tm9833)*; *sid-5(tm4328)* exhibited only a mild *bli-3* phenotype, indicating reduced sensitivity to feeding RNAi (Figure 3). Furthermore, no detectable phenotype was observed in *rexd-1(tm11388)*; *tbc-3(tm9833)*; *sid-5(tm4328)* triple mutant animals fed *bli-3* dsRNA food (Figure 3). These results suggest that REXD-1, TBC-3, and SID-5 act in parallel pathways for spreading dsRNA in systemic RNAi.

REXD-1, TBC-3, and SID-5 are required for systemic spreading of dsRNA but dispensable for dsRNA uptake into the intestine

Next, to test whether the *rexd-1(tm11388)*; *tbc-3(tm9833)*; *sid-5(tm4328)* triple mutant has resistance to feeding RNAi against genes expressed in other tissues, we fed the triple mutant animals bacteria expressing dsRNA targeting *pos-1*, *unc-15* and *act-5,* which are expressed in the germline, body wall muscles and intestine, respectively. Triple mutant animals were almost insensitive to *pos-1* and *unc-15* feeding RNAi, suggesting that their strong RNAi deficiency is not a tissue-specific phenotype (Figures 4A and 4B). However, triple mutant animals were affected upon *act-5* feeding RNAi, although they showed a milder phenotype than the wild type (Figure 4C). To determine whether the difference in silencing response between *act-5* and other genes was due to the tissue-specific effect or the difference in the amount of dsRNA required to silence them, we compared the RNAi response between the triple mutant and *rsd-3(tm9006)* mutant animals.[17] In contrast to the triple mutant, *rsd-3(tm9006)* mutants showed strong resistance to feeding RNAi against genes expressed in the intestine, whereas they were more sensitive to feeding RNAi than the triple mutant in other tissues (Figures S3A–S3E), indicating that the triple mutant is specifically sensitive to feeding RNAi in the intestine. These results suggest that REXD-1, TBC-3, and SID-5 are required for systemic spreading of dsRNA but dispensable for uptake of dsRNA into the intestine.

To examine whether spreading of silencing RNA derived from the transgene is also affected in the triple mutant, we used an integrated transgene expressing *gfp* hairpin RNA under the control of the *snb-1* promoter, which drives pan-neuronal gene expression as a dsRNA source, and another transgene that expresses nuclear-localized GFP in all somatic cells as a target of silencing. In the wild-type background, GFP expression that is particularly evident in the intestine was silenced by neuronal-derived dsRNA. In contrast, GFP expression was consistently detectable in the presence of the RNAi-inducible transgene in the triple mutant background (Figure 4D), indicating that REXD-1, TBC-3, and SID-5 also play important roles in the spread of transgene-derived dsRNA. On the other hand, GFP expression in intestinal cells was specifically sensitive to dietary supplied dsRNA in the triple mutant as well as in wild-type animals (Figures 4D, 4E, S3F, and S3G), which further confirms that uptake of dsRNA into the intestine is functional in the triple mutant animals.

REXD-1, TBC-3, and SID-5 are required for export of dsRNA from the intestine

In feeding RNAi, ingested dsRNA is first taken up by intestinal cells, subsequently exported into the pseudocoelom and then taken up by cells where it is processed and incorporated into the silencing machinery (Figure 5A). As the *rexd-1(tm11388)*; *tbc-3(tm9833)*; *sid-5(tm4328)* triple

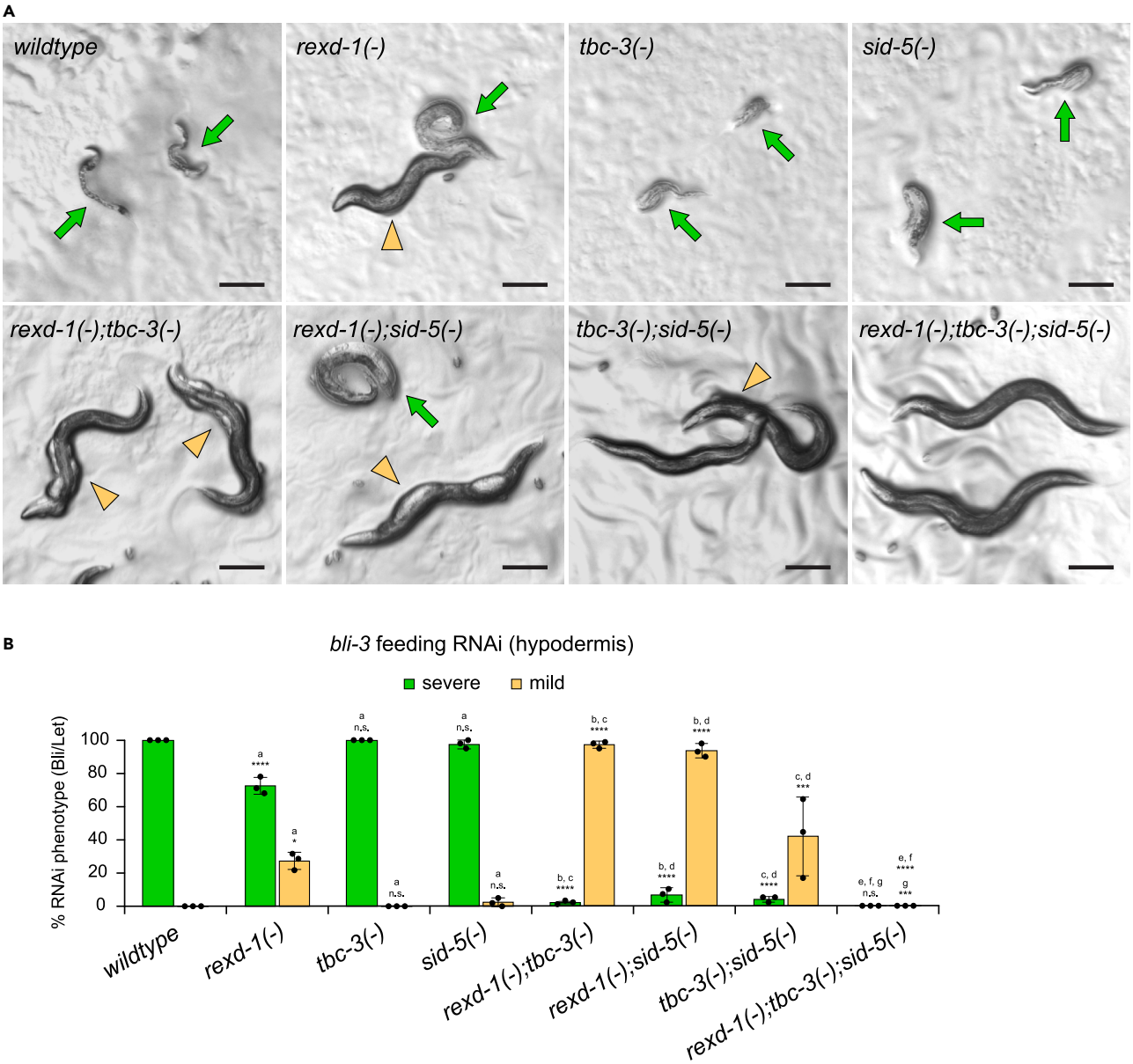

Figure 3. REXD-1, TBC-3 and SID-5 act in parallel pathways in systemic RNAi

(A) Representative images of the *bli-3* feeding RNAi assay. Green arrows indicate animals that showed the severe *bli-3* knockdown phenotype (larval lethal). Yellow arrowheads indicate gravid adult animals with blister (mild phenotype). Scale bars, 200 μm.

(B) Percentage of affected animals upon feeding RNAi against *bli-3*. Animals showed severe (larval lethal: Let) and mild (blister: Bli) *bli-3* knockdown phenotypes were separately scored. Bars represent the mean (±SEM) from three independent experiments. Genotypes of tested animals are indicated at the bottom. One-way ANOVA, Tukey's multiple comparison test. a, Comparison with the wild type. b, Comparison with *rexd-1(−)*. c, Comparison with *tbc-3(−)*. d, Comparison with *sid-5(−)*. e, Comparison with *rexd-1(−); tbc-3(−)*. f, Comparison with *rexd-1(−); sid-5(−)*. g, Comparison with *tbc-3(−); sid-5(−)*. ***p < 0.001, ****p < 0.0001, n.s. = not significant. Alleles used in Figure 3 are *rexd-1(−)*: *tm11388*, *tbc-3(−)*: *tm9833*, *sid-5(−)*: *tm4328*.

mutant showed strong resistance to feeding RNAi except for genes expressed in the intestine, we hypothesized that the RNAi defective phenotype in the triple mutant resulted from strong deficiency in the secretion of dsRNA from intestinal cells. To test whether the uptake of dsRNA and intracellular processing of dsRNA in the triple mutant are affected, we carried out microinjection of synthesized dsRNA targeting *pos-1* into the body cavity of animals, which allows dsRNA to spread throughout the body without intestinal export (Figure 5A). Injection of dsRNA into the pseudocoelom successfully induced RNAi knockdown of the target gene in the triple mutant as well as wild-type animals, whereas the *sid-1* mutant, which is defective in dsRNA import, showed resistance against injected dsRNA (Figure 5B). In contrast, as previously shown, triple mutant animals showed resistance to ingested *pos-1* dsRNA that is comparable to *sid-1* mutant animals (Figure 5B). These

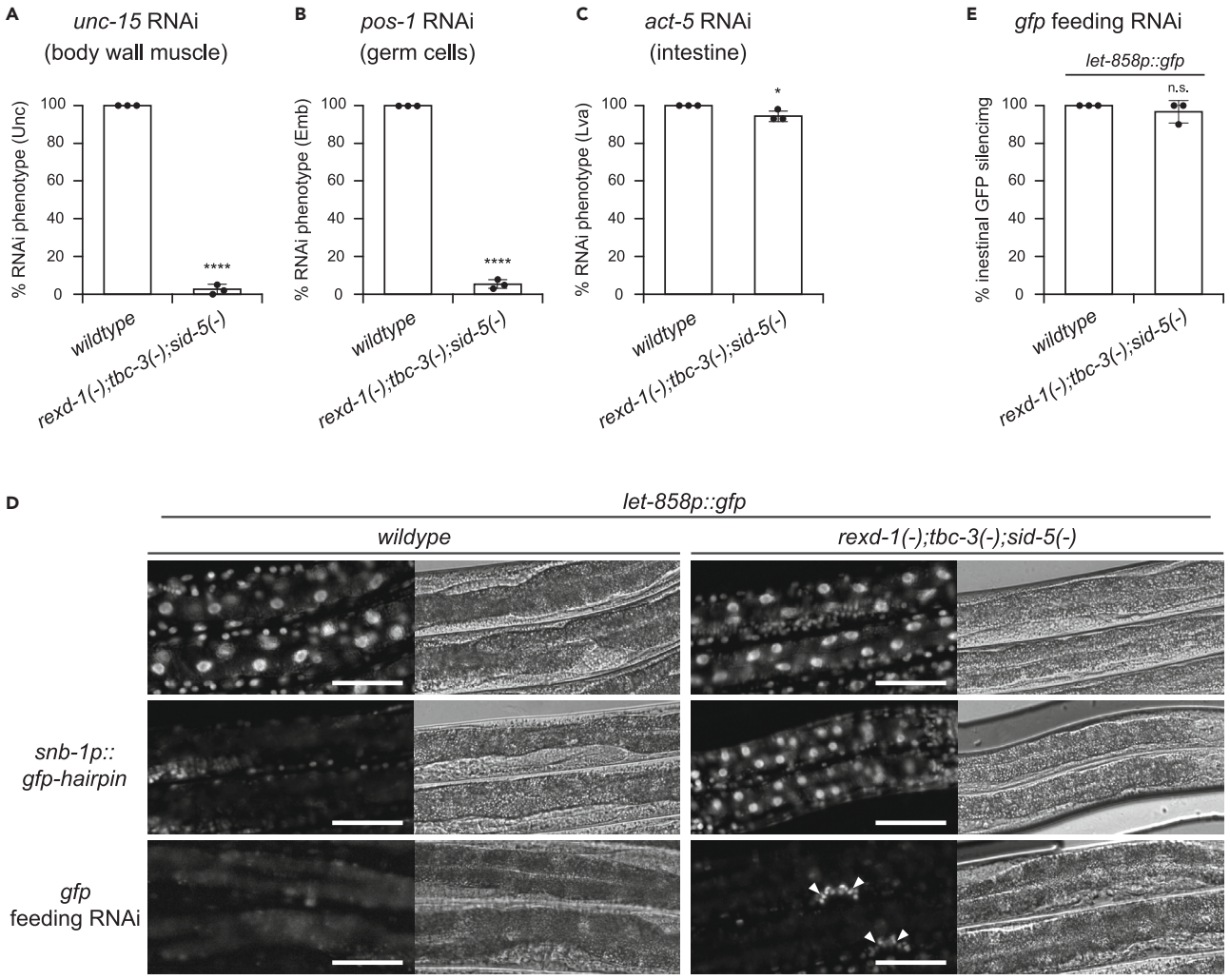

Figure 4. REXD-1, TBC-3 and SID-5 are required for systemic RNAi but dispensable for uptake of dsRNA into the intestine

(A–C) Percentage of animals that showed the uncoordinated (Unc) phenotype upon feeding RNAi against the body wall muscle-expressed gene *unc-15* (A), percentage of embryonic lethality (Emb) of F1 progeny of animals fed bacteria expressing dsRNA against the germline-expressed gene *pos-1* (B), and percentage of animals that showed the larval arrest (Lva) phenotype upon feeding RNAi against the intestinal gene *act-5* (C).

(D) Images of L4 animals possessing the *let-858p::gfp* transgene, which expresses nuclear localized GFP in all somatic cells, in wild-type (left) and *rexd-1(−); tbc-3(−); sid-5(−)* triple mutant (right) background. In each genotype, fluorescence images for GFP are on the left and differential interference contrast images are on the right. Images of untreated animals are on the top. Images of animals carrying an additional transgene which expresses neuronal *gfp-hairpin*, are on the middle. Images of animals fed bacteria expressing dsRNA against *gfp* are on the bottom. Arrowheads indicate GFP expression in the vulval epithelium. Scale bars, 50 μm.

(E) Percentage of animals with silenced intestinal GFP expression derived from the *let-858p::gfp* transgene upon feeding RNAi against *gfp*. Bars represent the mean (±SEM) from three independent experiments. Two-tailed t-test. *p < 0.05, ****p < 0.0001, n.s. = not significant. Alleles used in Figure 4 are *rexd-1(−)*: *tm11388*, *tbc-3(−)*: *tm9833*, *sid-5(−)*: *tm4328*. See also Figure S3.

results indicate that neither deficiency in the import of dsRNA nor inability of intracellular processing of dsRNA is a major reason for systemic RNAi defects in the triple mutant and support our hypothesis that export of dsRNA from the intestine is strongly perturbed in the triple mutant. To test whether REXD-1, TBC-3, and SID-5 function in independent pathways for dsRNA secretion, we expressed these factors in the intestine of the triple mutant. Intestine-specific expression of REXD-1, TBC-3, or SID-5 partially restored sensitivity to feeding dsRNA in the triple mutant background, suggesting that REXD-1, TBC-3, and SID-5 act in parallel pathways and promote export of dsRNA from the intestine (Figures S4A–S4C).

We next asked whether secretion from the intestine is generally perturbed in the triple mutant. The yolk protein VIT-2 is expressed in and secreted from the intestine and imported to oocytes. We used a transgene expressing VIT-2 fused with GFP[33] and found no obvious defect in the transport of VIT-2::GFP from the intestine to the oocyte in the triple mutant background (Figure S4D). This is consistent with the fact that triple mutant animas show no obvious developmental defect and produce viable progeny. In aged worms, *mir-83* is expressed in the intestine,

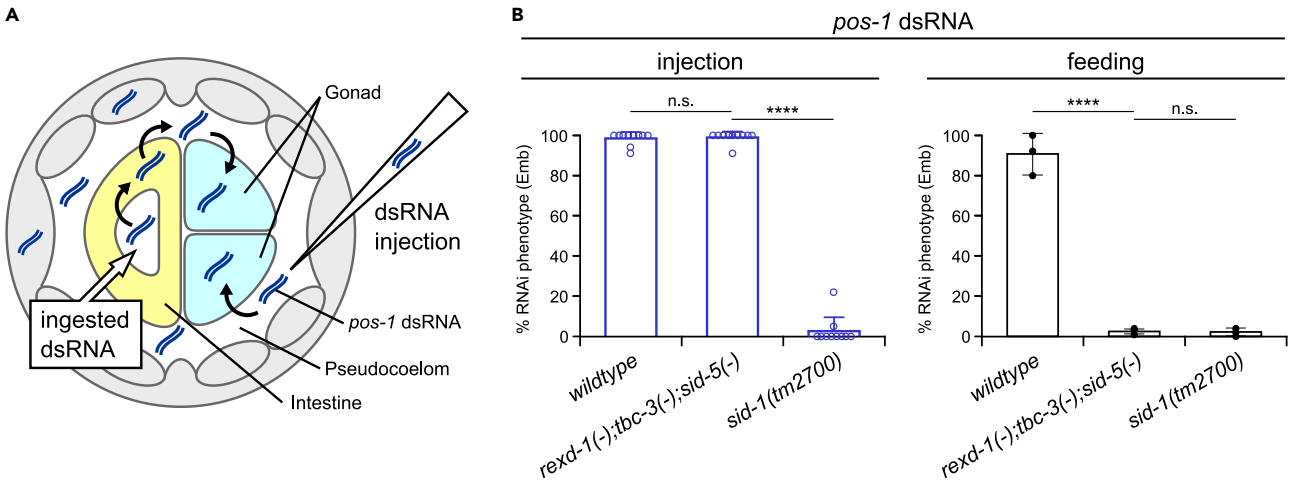

Figure 5. REXD-1, TBC-3 and SID-5 are required for export of dsRNA from the intestine

(A) Schematic illustration of dsRNA spreading across tissues during feeding RNAi and pseudocoelomic injection of dsRNA. A cross section of the *C. elegans* body is shown.

(B) Response to dsRNA against the germline-expressed gene *pos-1* introduced by the pseudocoelomic injection (left) and the ingestion (right) in wild type, *rexd-1(−); tbc-3(−); sid-5(−)* triple mutant and *sid-1(tm2700)*. In the dsRNA injection experiment, the percentage of embryonic lethality (Emb) of the F1 progeny of each injected animal was scored. Bars represent the average of ten animals for each genotype. For the feeding RNAi experiment, the percentage of Emb of the F1 progeny of animals fed *pos-1* dsRNA food was scored. Bars represent the mean (±SEM) from three independent experiments. One-way ANOVA, Tukey's multiple comparison test. ****$p < 0.0001$, n.s. = not significant. See also Figure S4.

transported across tissues and suppresses *cup-5* expression, resulting in decreased autophagy and enlargement of LMP-1-labeled vesicles in coelomocytes.[34] If secretion of *mir-83* was disrupted, LMP-1-positive vesicles should be smaller than normal due to the suppression of enlargement, as in the *mir-83* mutant.[34] Enlarged LMP-1-positive vesicles were observed in the aged coelomocytes in the triple mutant background (Figure S4E), implying that secretion of *mir-83* from the intestine is not impaired. These results suggest that REXD-1, TBC-3, and SID-5 are likely to be specifically required for the export of dsRNA rather than for general secretion events from the intestine.

Activation of UNC-108/Rab-2 negatively regulates systemic RNAi

To further understand the regulatory mechanism of dsRNA secretion, we focused our attention on TBC-3, which is an evolutionally conserved regulator of vesicle trafficking. TBC family proteins regulate membrane traffic by activating GTP hydrolysis by Rab GTPases to convert the active GTP-bound form into the inactive GDP-bound form of Rabs (Figure S5A).[29,30] To determine if TBC-3 is involved in systemic RNAi as a RabGAP, we expressed a catalytically inactivated form of TBC-3b (RQ-AA) in *tbc-3(tm9833)* animals. The inactivated form of TBC-3 failed to rescue the RNAi deficiency in *tbc-3(tm9833)* mutants (Figure S5B), suggesting that the GAP activity of TBC-3 is required to regulate systemic RNAi. Then, we next determined which Rab protein is the target of TBC-3. TBC1D22A and TBC1D22B, human orthologs of *C. elegans* TBC-3, are referred to as Rab33 GAP,[32] since the TBC domain of Gyp1p, a yeast ortholog of TBC1D22A and TBC1D22B, displays high selectivity for mammalian Rab33 as a substrate.[35] On the other hand, in *Drosophila*, dTBC1D22 functions as a Rab40 GAP to regulate lipid homeostasis.[36] As its target Rab is expected to be abnormally activated in TBC-3-deficient animals, inactivation of the target Rab will lead to suppression of the phenotype in the *tbc-3* mutant. We generated double mutant animals harboring *tbc-3(tm9833)* and *rab-33(tm2641)* or *rabr-1(tm2564)* encoding a Rab40-like protein according to OrthoList2.[37] Both *rab-33(tm2641); tbc-3(tm9833)* and *tbc-3(tm9833); rabr-1(tm2564)* double mutant animals showed partial resistance to *bli-1* feeding RNAi, which is comparable to the *tbc-3* single mutant (Figures S5C and S5D). These results indicate that TBC-3 acts as a GAP for a RAB protein other than RAB-33 and RABR-1 in systemic RNAi regulation. We next performed an RNAi screen targeting *C. elegans rab* genes, but no suppressor of *tbc-3* was identified (Table S1).

To identify interactors of TBC-3 in systemic RNAi regulation, we performed a genetic screen for mutants that suppress RNAi deficiency in *tbc-3(tm9833)*. Interestingly, we identified a recessive mutation in *unc-108(tm9924)*, which encodes the *C. elegans* ortholog of Rab2, as a suppressor of *tbc-3*. The *unc-108(tm9924)* mutation increases sensitivity to *bli-1* and *pos-1* feeding RNAi in *tbc-3(tm9833)*, and expression of *unc-108* reversed the effect of the *unc-108(tm9924)* mutation (Figures 6A and 6B). We next tested a loss-of-function allele of *unc-108(n3263)*[38] and found that *unc-108(n3263); tbc-3(tm9833)* double mutant animals are more sensitive to feeding RNAi than *tbc-3(tm9833)* single mutants, which is similar to the suppressor strain harboring *unc-108(tm9924)* (Figure 6C). These results indicate that inactivation of UNC-108 suppresses *tbc-3(tm9833)* RNAi deficiency. We also found that *unc-108(n3263)* single mutant animals were more sensitive to *lin-1* feeding RNAi than wild-type animals (Figure 6D), suggesting that UNC-108 activity antagonizes systemic RNAi silencing.

To further examine the effect of UNC-108 activity on systemic RNAi regulation, we next tested a mutant of *gop-1(tm5384)*, which encodes a UNC-108 activating protein.[39] *gop-1(tm5384); tbc-3(tm9833)* double mutant animals showed increased sensitivity to feeding RNAi compared with *tbc-3(tm9833)* single mutants, as seen in *unc-108; tbc-3* double mutants (Figures 6E and 6F). Similar to *unc-108(n3263)*, *gop-1(tm5384)*

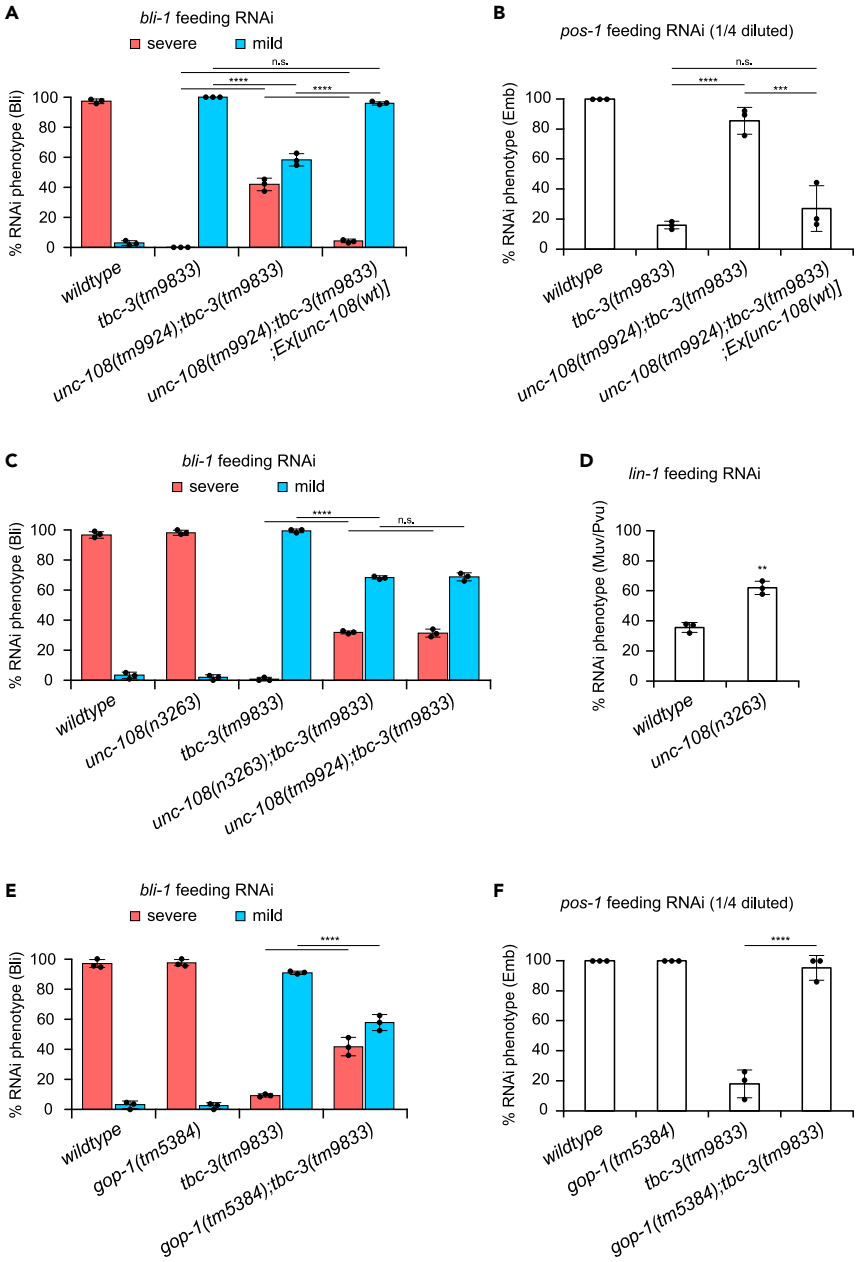

Figure 6. Reducing UNC-108/Rab-2 activity restores RNAi sensitivity in *tbc-3* mutants

(A, C, and E) Percentage of affected animals upon *bli-1* feeding RNAi. Animals showed severe and mild blister (Bli) phenotypes were separately scored.

(B and F) Percentage of embryonic lethality (Emb) of F1 progeny of animals fed *pos-1* dsRNA food.

(D) Percentage of affected animals upon *lin-1* feeding RNAi in wild type and *unc-108(n3263)*. Animals showed multi-vulva (Muv) or protruding vulva (Pvu) phenotypes were scored. Bars represent the mean (±SEM) from three independent experiments. Genotypes and introduced transgenes of tested animals are indicated at the bottom. One-way ANOVA, Tukey's multiple comparison test (A–C, E, F) or two-tailed t-test (D). **p < 0.01, ***p < 0.001, ****p < 0.0001, n.s. = not significant. See also Figure S5 and Table S1.

single mutants were also more sensitive to *lin-1* RNAi by feeding than wild-type animals (Figure S5E). These results confirm that reduced activation of UNC-108 suppresses RNAi deficiency in *tbc-3(tm9833)* mutants and that the activity of UNC-108 negatively regulates systemic RNAi. UNC-108 interacts and acts together with an effector, RIC-19, and two binding proteins, RUND-1 and CCCP-1, to regulate dense-core vesicle maturation.[40,41] We examined the efficacy of *lin-1* feeding RNAi in *ric-19(ok833)*, *rund-1(tm3622)* and *cccp-1(ox334)* mutant animals. Among these UNC-108 interactor mutants, only *rund-1(tm3622)* mutants showed enhanced sensitivity to *lin-1* RNAi (Figure S5F), suggesting that UNC-108 interactors partially overlap but are different between systemic RNAi and dense-core vesicle regulation.

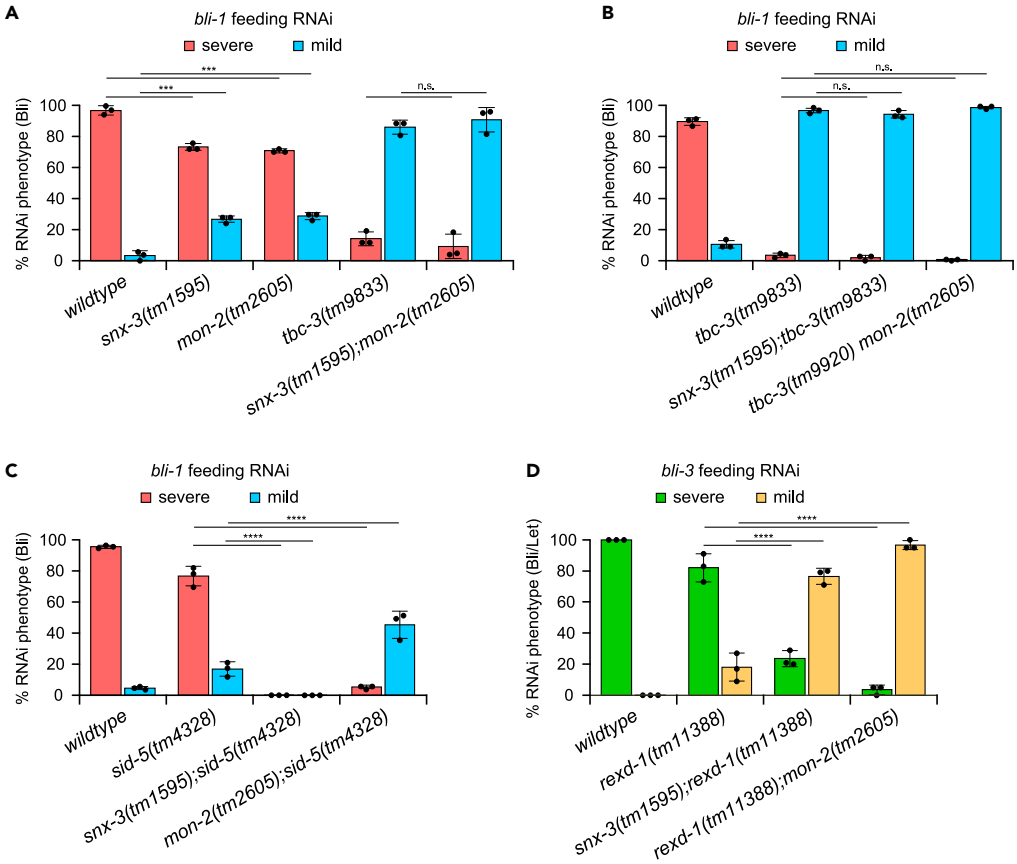
A
bli-1 feeding RNAi
severe
mild
% RNAi phenotype (Bli)
wildtype
snx-3(tm1595)
mon-2(tm2605)
tbc-3(tm9833)
snx-3(tm1595);mon-2(tm2605)
B
bli-1 feeding RNAi
severe
mild
% RNAi phenotype (Bli)
wildtype
tbc-3(tm9833)
snx-3(tm1595);tbc-3(tm9833)
tbc-3(tm9920) mon-2(tm2605)
C
bli-1 feeding RNAi
severe
mild
% RNAi phenotype (Bli)
wildtype
sid-5(tm4328)
snx-3(tm1595);sid-5(tm4328)
mon-2(tm2605);sid-5(tm4328)
D
bli-3 feeding RNAi
severe
mild
% RNAi phenotype (Bli/Let)
wildtype
rexd-1(tm11388)
snx-3(tm1595);rexd-1(tm11388)
rexd-1(tm11388);mon-2(tm2605)

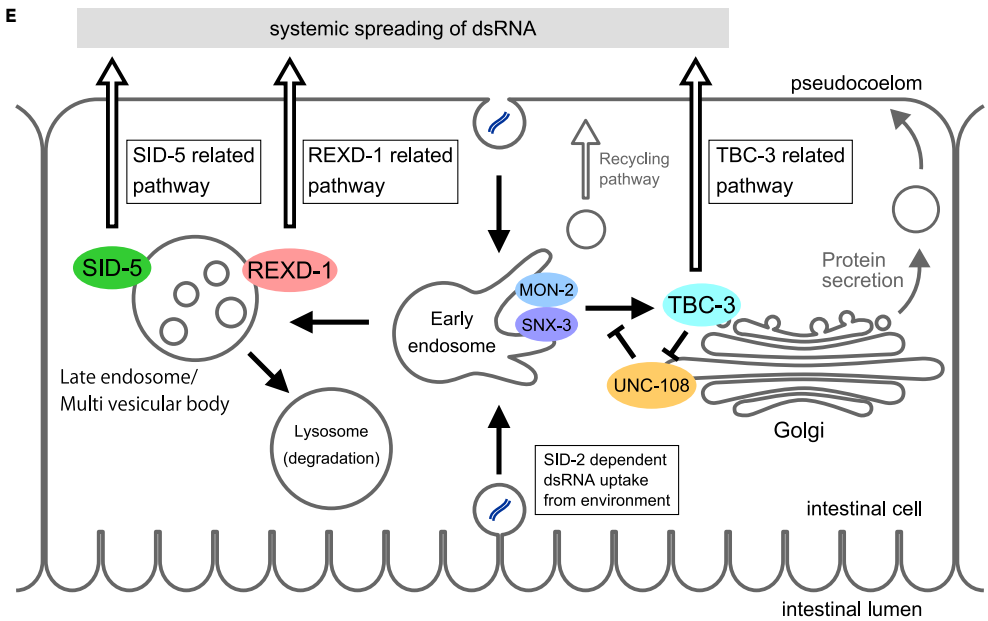
E
systemic spreading of dsRNA
pseudocoelom
SID-5 related pathway
REXD-1 related pathway
Recycling pathway
TBC-3 related pathway
SID-5
REXD-1
Protein secretion
MON-2
SNX-3
Early endosome
TBC-3
Late endosome/
Multi vesicular body
UNC-108
Golgi
Lysosome
(degradation)
SID-2 dependent dsRNA uptake from environment
intestinal cell
intestinal lumen

Figure 7. SNX-3 and MON-2 act in the TBC-3-related pathway to regulate systemic RNAi

(A–C) Percentage of affected animals upon *bli-1* feeding RNAi. Animals showed severe and mild blister (Bli) phenotypes were separately scored.

(D) Percentage of affected animals upon *bli-3* feeding RNAi. Animals showed severe (larval lethal: Let) and mild (blister: Bli) *bli-3* knockdown phenotypes were separately scored.

(E) Proposed model for dsRNA export regulated by distinct pathways.

(A–D) Bars represent the mean (±SEM) from three independent experiments. Genotypes of tested animals are indicated at the bottom. One-way ANOVA, Tukey's multiple comparison test. ***p < 0.001, ****p < 0.0001, n.s. = not significant.

Our observation that inactivation of UNC-108 suppresses TBC-3 deficiency suggests the possibility that UNC-108 is the inactivation target of TBC-3 in systemic RNAi regulation. As *unc-108* mutation did not completely suppress *tbc-3* (Figure 6C), it is still possible that there is another Rab(s) redundantly acting with UNC-108. In the *C. elegans* genome, there are tandemly aligned *rab-related* genes, *rabr-3* and *rabr-4*, both of which encode proteins closely related to Rab2.[42] We generated the deletion allele *tm9826* that removes both *rabr-3* and *rabr-4*. Simultaneous disruption of *rabr-3* and *rabr-4* did not affect RNAi sensitivity (Figure S5G), indicating that RABR-3 and RABR-4 functions are dispensable for systemic RNAi regulation. Phylogenetic analysis suggests that Rab14 and Rab4, which is lost in *C. elegans,* are neighboring paralogs of Rab2 among Rab GTPases.[43] In *C. elegans*, RAB-14 and UNC-108 redundantly regulate phagosome maturation during apoptotic cell clearance.[44] *rab-14(tm2095)* mutant animals showed RNAi sensitivity similar to that of wild-type animals, whereas *unc-108(n3263)* mutants showed increased sensitivity (Figure S5H), suggesting that unlike in phagosome maturation, UNC-108 and RAB-14 do not function redundantly in systemic RNAi. These results support the specificity of UNC-108 function in systemic RNAi regulation.

Membrane trafficking between endosomes and the Golgi appears to be a part of the TBC-3-related pathway in systemic RNAi

To further characterize the membrane trafficking pathway that TBC-3 regulates in systemic RNAi, we decided to use mutants for defined regulators of vesicular transport. We tested mutants of SNX-3 and MON-2, which are required for the retrograde trafficking of Wntless/MIG-14 between endosomes and the Golgi,[45,46] since previous studies reported that the disruption of SNX-3, MON-2 and TBC-3 functions causes similar phenotypes, reducing the long lifespan of *isp-1* mutants[47] and suppressing impaired asymmetric cell division of seam cells in the *ipla-1* mutant.[31] Single mutants of *snx-3(tm1595)* and *mon-2(tm2605)* were sensitive to *bli-1* feeding RNAi but less sensitive than the wild type (Figure 7A). To examine whether SNX-3 and MON-2 act redundantly in systemic RNAi regulation, we generated an *snx-3(tm1595); mon-2(tm2605)* double mutant. *snx-3(tm1595); mon-2(tm2605)* animals showed resistance to *bli-1* feeding RNAi similar to the *tbc-3* mutant (Figure 7A), suggesting that SNX-3 and MON-2 act redundantly to regulate systemic RNAi. To investigate whether SNX-3 and MON-2 act in the same pathway as TBC-3, we constructed animals harboring the *tbc-3* mutation and *snx-3* or *mon-2* mutation. As *tbc-3* and *mon-2* are located closely on the same chromosome, we generated a deletion allele, *tbc-3(tm9920)*, in the *mon-2(tm2605)* background by CRISPR (Figure S2A). Both *snx-3(tm1595); tbc-3(tm9833)* and *tbc-3(tm9920) mon2(tm2605)* double mutants showed partial resistance to feeding RNAi comparable to *tbc-3* single mutants (Figure 7B). This suggests that SNX-3 and MON-2 act upstream of TBC-3 in the same pathway to regulate systemic RNAi. In contrast, RNAi resistance in both *rexd-1(tm11388)* and *sid-5(tm4328)* mutants was enhanced by introducing mutations of either *snx-3(tm1595)* or *mon-2(tm2605)* (Figures 7C and 7D). This further confirms that REXD-1, SID-5, and TBC-3 act in distinct pathways to regulate the transport of silencing RNA.

DISCUSSION

In the present study, we identified REXD-1 and TBC-3 as novel players in regulating systemic RNAi. We showed that both REXD-1 and TBC-3 can promote systemic RNAi silencing in a non-cell autonomous manner and that these two factors and another non-cell autonomous factor, SID-5, act redundantly in systemic RNAi. We found that triple mutant animals lacking REXD-1, TBC-3, and SID-5 functions are strongly resistant to RNAi triggered by ingested dsRNA, with the exception of intestinal cells, but sensitive to dsRNA injected into the body cavity. Furthermore, the triple mutant animals also showed deficiency in spreading dsRNA expressed in neurons. From these observations, we conclude that REXD-1, TBC-3, and SID-5 constitute distinct pathways to regulate the export of dsRNA out of cells during systemic RNAi (Figure 7E). As *rexd-1; tbc-3; sid-5* triple mutant animals show weak resistance to feeding RNAi in the intestine, it is possible that these factors are dispensable but involved in other steps during systemic RNAi, such as the cytosolic uptake, processing of dsRNA and amplifying silencing signals. Although we used the mutants of secretory Rabs, *aex-6* and *rab-3*, for our genetic screen, RNAi deficiency in *rexd-1* and *tbc-3* mutants, which we identified, seemed not to depend on the mutations of *aex-6* and *rab-3*. This is consistent with our notion that dsRNA export out of cells is separately regulated from general secretion events, e.g., secretion of yolk proteins.

REXD-1 seemed to be located in the cytosol and associate with late endosomes and lysosomes, which requires an isoform-specific 78 AA length domain. The association with endosomal compartments and/or the isoform-specific domain itself are required for REXD-1 function to regulate systemic RNAi, since the shorter isoform that is not located in the cytoplasm failed to rescue the RNAi deficiency. SID-5 is also reported to associate with late endosomes marked by GFP::RAB-7 and LMP-1::GFP.[19] Late endosomes, also referred to as multivesicular bodies (MVBs), fuse with the plasma membrane to release exosomes, extracellular vesicles that have been shown to contain mRNAs and microRNAs.[48] Thus, it is possible that REXD-1 promotes MVB-mediated export of dsRNA in a distinct way to SID-5 (Figure 7E). Alternatively, REXD-1 may prevent MVB fusion with lysosomes. A conserved SNARE, SEC-22, is suggested to negatively regulate systemic RNAi by promoting fusion between MVBs and lysosomes.[49] If REXD-1 prevents dsRNA from lysosomal degradation, it is possible that REXD-1 facilitates both

systemic spreading and cell autonomous RNAi silencing, which could explain why both intestine- and target tissue-specific expression of REXD-1 can rescue RNAi deficiency in *rexd-1* mutants. As no membrane-associated domain is predicted, REXD-1 is likely to interact with other protein(s) to associate with endosomes and to regulate the transport of dsRNA. Identification of REXD-1 interactors in future work will be necessary to understand the mechanism by which dsRNA transport is regulated.

In addition to late endosome/MVB-mediated export, we demonstrated that endosome-to-Golgi trafficking mediated by TBC-3 is involved in the secretion of dsRNA during systemic RNAi. Our genetic interaction assay suggests that TBC-3 acts downstream of SNX-3 and MON-2. SNX-3 acts with a retromer cargo-selective subcomplex and a membrane remodeling complex containing MON-2 to mediate recycling of endocytosed Wntless.[45,46,50] It is thus suggested that transport of dsRNA also involves retromer-mediated trafficking similar to the sorting of Wntless. TBC domain-containing proteins regulate vesicle trafficking pathways by inactivating Rab GTPases. A series of observations suggest that UNC-108/Rab2 is a strong candidate substrate for TBC-3 to regulate dsRNA transport. First, loss of UNC-108 function led to the suppression of the RNAi defective phenotype in *tbc-3* mutants. Second, disruption of UNC-108 as well as its activator and interactor enhanced sensitivity to feeding RNAi. Third, other candidates, including previously reported targets Rabs, RAB-33 and RAB-40, and Rab2-related factors, did not seem to be involved in systemic RNAi regulation. It has been reported that knockdown of *unc-108* suppresses QL.d migration defects caused by disruption of Wntless recycling and reduced Wnt secretion in mutants of the retromer subunit *vps-29*.[51] We therefore propose that UNC-108 activity plays an opposing role (likely promoting degradation) to dsRNA transport mediated by endosome-to-Golgi trafficking, where TBC-3 acts during systemic RNAi (Figure 7E).

Although our results suggest that REXD-1, TBC-3, and SID-5 constitute major pathways for the export of dsRNA, there are probably additional pathways to mediate dsRNA secretion. For example, it has been suggested that basolateral recycling mediated by sequential protein interactions between EHBP-1, SID-3, NCK-1 and DYN-1 is involved in the export of ingested dsRNA.[52] The existence of pathways acting in parallel to dsRNA secretion enables stable systemic transport of dsRNA. A recent study reported that a small noncoding RNA expressed in a pathogenic bacterium, *Pseudomonas aeruginosa* (PA14), induces heritable learning in worms to avoid this pathogen.[53] This requires transport of bacterial RNA between the gut and germlines in a SID-1- and SID-2-dependent manner. It is thus suggested that the robust mechanism for systemic spreading of dsRNA is important to utilize RNA molecules as environmental information, allowing animals to adapt their physiology to their environment.

Limitations of the study

We proposed a model in which REXD-1, TBC-3, and SID-5 play important roles in regulating systemic RNAi in dsRNA donor cells (Figure 7E). This model does not exclude the potential role of these factors in dsRNA recipient cells to modulate the efficiency of RNAi. It is possible that REXD-1, TBC-3, and SID-5 play additional and/or cell type-specific roles in processes other than dsRNA secretion during systemic RNAi, such as the cytosolic uptake of dsRNA, processing of dsRNA and amplification of silencing signals. It will be important to dissect the functions of these factors during systemic RNAi in future studies.

STAR★METHODS

Detailed methods are provided in the online version of this paper and include the following:

- KEY RESOURCES TABLE
- RESOURCE AVAILABILITY
  - Lead contact
  - Materials availability
  - Data and code availability
- EXPERIMENTAL MODEL AND STUDY PARTICIPANT DETAILS
- METHOD DETAILS
  - Forward genetic screens
  - Whole-genome sequencing and mutation mapping
  - CRISPR/Cas9-mediated genome editing
  - Generation of transgenic animals
  - RNAi experiments
  - Microscopy
- QUANTIFICATION AND STATISTICAL ANALYSIS

SUPPLEMENTAL INFORMATION

Supplemental information can be found online at https://doi.org/10.1016/j.isci.2023.108067.

ACKNOWLEDGMENTS

We thank Dr. Rieko Imae for constructing *tmIs1059*, the Medical Research Institute (MRI) of Tokyo Women's Medical University for undertaking confocal microscopy and the Mitani lab members for their support. Some strains were provided by the CGC, which is funded by NIH Office

445 of Research Infrastructure Programs (P40 OD010440). This work was supported by JSPS KAKENHI Grant Number JP18K15015 to K.Y. and Grant Numbers JP16H05123 and JP20H03422 to S.M.

AUTHOR CONTRIBUTIONS

Conceptualization, K.Y. and S.M.; Investigation, K.Y., Y.S., K.D., and S.Y.; Writing – Original Draft, K.Y.; Writing – Review and Editing, K.Y., Y.S., K.D., S.Y., and S.M.; Funding Acquisition, K.Y. and S.M.

DECLARATION OF INTERESTS

The authors declare no competing interests.

Received: June 15, 2023
Revised: September 8, 2023
Accepted: September 25, 2023
Published: September 28, 2023

REFERENCES

1. Fire, A., Xu, S., Montgomery, M.K., Kostas, S.A., Driver, S.E., and Mello, C.C. (1998). Potent and specific genetic interference by double-stranded RNA in Caenorhabditis elegans. Nature *391*, 806–811. https://doi.org/10.1038/35888.
2. Winston, W.M., Molodowitch, C., and Hunter, C.P. (2002). Systemic RNAi in C. elegans Requires the Putative Transmembrane Protein SID-1. Science *295*, 2456–2459. https://doi.org/10.1126/science.1068836.
3. Tabara, H., Grishok, A., and Mello, C.C. (1998). RNAi in C. elegans: Soaking in the Genome Sequence. Science *282*, 430–431. https://doi.org/10.1126/science.282.5388.430.
4. Timmons, L., and Fire, A. (1998). Specific interference by ingested dsRNA. Nature *395*, 854. https://doi.org/10.1038/27579.
5. Fraser, A.G., Kamath, R.S., Zipperlen, P., Martinez-Campos, M., Sohrmann, M., and Ahringer, J. (2000). Functional genomic analysis of C. elegans chromosome I by systematic RNA interference. Nature *408*, 325–330. https://doi.org/10.1038/35042517.
6. Kamath, R.S., Martinez-Campos, M., Zipperlen, P., Fraser, A.G., and Ahringer, J. (2001). Effectiveness of specific RNA-mediated interference through ingested double-stranded RNA in Caenorhabditis elegans. Genome Biol. *2*. RESEARCH0002. https://doi.org/10.1186/gb-2000-2-1-research0002.
7. Kamath, R.S., Fraser, A.G., Dong, Y., Poulin, G., Durbin, R., Gotta, M., Kanapin, A., Le Bot, N., Moreno, S., Sohrmann, M., et al. (2003). Systematic functional analysis of the Caenorhabditis elegans genome using RNAi. Nature *421*, 231–237. https://doi.org/10.1038/nature01278.
8. Maeda, I., Kohara, Y., Yamamoto, M., and Sugimoto, A. (2001). Large-scale analysis of gene function in Caenorhabditis elegans by high-throughput RNAi. Curr. Biol. *11*, 171–176. https://doi.org/10.1016/s0960-9822(01)00052-5.
9. Tabara, H., Yigit, E., Siomi, H., and Mello, C.C. (2002). The dsRNA Binding Protein RDE-4 Interacts with RDE-1, DCR-1, and a DExH-Box Helicase to Direct RNAi in C. elegans. Cell *109*, 861–871. https://doi.org/10.1016/S0092-8674(02)00793-6.
10. Tijsterman, M., May, R.C., Simmer, F., Okihara, K.L., and Plasterk, R.H.A. (2004). Genes Required for Systemic RNA Interference in Caenorhabditis elegans. Curr. Biol. *14*, 111–116. https://doi.org/10.1016/j.cub.2003.12.029.
11. Feinberg, E.H., and Hunter, C.P. (2003). Transport of dsRNA into Cells by the Transmembrane Protein SID-1. Science *301*, 1545–1547. https://doi.org/10.1126/science.1087117.
12. Jose, A.M., Smith, J.J., and Hunter, C.P. (2009). Export of RNA silencing from C. elegans tissues does not require the RNA channel SID-1. Proc. Natl. Acad. Sci. USA *106*, 2283–2288. https://doi.org/10.1073/pnas.0809760106.
13. Winston, W.M., Sutherlin, M., Wright, A.J., Feinberg, E.H., and Hunter, C.P. (2007). *Caenorhabditis elegans* SID-2 is required for environmental RNA interference. Proc. Natl. Acad. Sci. USA *104*, 10565–10570. https://doi.org/10.1073/pnas.0611282104.
14. McEwan, D.L., Weisman, A.S., and Hunter, C.P. (2012). Uptake of Extracellular Double-Stranded RNA by SID-2. Mol. Cell *47*, 746–754. https://doi.org/10.1016/j.molcel.2012.07.014.
15. Jose, A.M., Kim, Y.A., Leal-Ekman, S., and Hunter, C.P. (2012). Conserved tyrosine kinase promotes the import of silencing RNA into *Caenorhabditis elegans* cells. Proc. Natl. Acad. Sci. USA *109*, 14520–14525. https://doi.org/10.1073/pnas.1201153109.
16. Bhatia, S., and Hunter, C.P. (2022). SID-4/NCK-1 is important for dsRNA import in Caenorhabditis elegans. G3 (Bethesda) *12*, jkac252. https://doi.org/10.1093/g3journal/jkac252.
17. Imae, R., Dejima, K., Kage-Nakadai, E., Arai, H., and Mitani, S. (2016). Endomembrane-associated RSD-3 is important for RNAi induced by extracellular silencing RNA in both somatic and germ cells of Caenorhabditis elegans. Sci. Rep. *6*, 28198. https://doi.org/10.1038/srep28198.
18. Saleh, M.-C., van Rij, R.P., Hekele, A., Gillis, A., Foley, E., O'Farrell, P.H., and Andino, R. (2006). The endocytic pathway mediates cell entry of dsRNA to induce RNAi silencing. Nat. Cell Biol. *8*, 793–802. https://doi.org/10.1038/ncb1439.
19. Hinas, A., Wright, A.J., and Hunter, C.P. (2012). SID-5 Is an Endosome-Associated Protein Required for Efficient Systemic RNAi in C. elegans. Curr. Biol. *22*, 1938–1943. https://doi.org/10.1016/j.cub.2012.08.020.
20. Jose, A.M. (2015). Movement of regulatory RNA between animal cells: I ntercellular RNA. genesis *53*, 395–416. https://doi.org/10.1002/dvg.22871.
21. Stenmark, H. (2009). Rab GTPases as coordinators of vesicle traffic. Nat. Rev. Mol. Cell Biol. *10*, 513–525. https://doi.org/10.1038/nrm2728.
22. Fukuda, M. (2008). Membrane traffic in the secretory pathway: Regulation of secretory vesicle traffic by Rab small GTPases. Cell. Mol. Life Sci. *65*, 2801–2813. https://doi.org/10.1007/s00018-008-8351-4.
23. Cao, J., Packer, J.S., Ramani, V., Cusanovich, D.A., Huynh, C., Daza, R., Qiu, X., Lee, C., Furlan, S.N., Steemers, F.J., et al. (2017). Comprehensive single-cell transcriptional profiling of a multicellular organism. Science *357*, 661–667. https://doi.org/10.1126/science.aam8940.
24. Treusch, S., Knuth, S., Slaugenhaupt, S.A., Goldin, E., Grant, B.D., and Fares, H. (2004). Caenorhabditis elegans functional orthologue of human protein h-mucolipin-1 is required for lysosome biogenesis. Proc. Natl. Acad. Sci. USA *101*, 4483–4488. https://doi.org/10.1073/pnas.0400709101.
25. Hermann, G.J., Schroeder, L.K., Hieb, C.A., Kershner, A.M., Rabbitts, B.M., Fonarev, P., Grant, B.D., and Priess, J.R. (2005). Genetic Analysis of Lysosomal Trafficking in Caenorhabditis elegans. Mol. Biol. Cell *16*, 3273–3288. https://doi.org/10.1091/mbc.e05-01-0060.
26. Chen, C.C.-H., Schweinsberg, P.J., Vashist, S., Mareiniss, D.P., Lambie, E.J., and Grant, B.D. (2006). RAB-10 Is Required for Endocytic Recycling in the Caenorhabditis elegans Intestine. Mol. Biol. Cell *17*, 1286–1297. https://doi.org/10.1091/mbc.e05-08-0787.
27. Yang, H., Zhang, Y., Vallandingham, J., Li, H., Florens, L., and Mak, H.Y. (2012). The RDE-10/RDE-11 complex triggers RNAi-induced mRNA degradation by association with target mRNA in *C. elegans*. Genes Dev. *26*, 846–856. https://doi.org/10.1101/gad.180679.111.
28. Zhang, C., Montgomery, T.A., Fischer, S.E.J., Garcia, S.M.D.A., Riedel, C.G., Fahlgren, N., Sullivan, C.M., Carrington, J.C., and Ruvkun, G. (2012). The Caenorhabditis elegans RDE-10/RDE-11 Complex Regulates RNAi by

Promoting Secondary siRNA Amplification. Curr. Biol. *22*, 881–890. https://doi.org/10.1016/j.cub.2012.04.011.

29. Fukuda, M. (2011). TBC proteins: GAPs for mammalian small GTPase Rab? Biosci. Rep. *31*, 159–168. https://doi.org/10.1042/BSR20100112.
30. Müller, M.P., and Goody, R.S. (2018). Molecular control of Rab activity by GEFs, GAPs and GDI. Small GTPases *9*, 5–21. https://doi.org/10.1080/21541248.2016.1276999.
31. Kanamori, T., Inoue, T., Sakamoto, T., Gengyo-Ando, K., Tsujimoto, M., Mitani, S., Sawa, H., Aoki, J., and Arai, H. (2008). β-Catenin asymmetry is regulated by PLA1 and retrograde traffic in C. elegans stem cell divisions. EMBO J. *27*, 1647–1657. https://doi.org/10.1038/emboj.2008.102.
32. Yue, X., Bao, M., Christiano, R., Li, S., Mei, J., Zhu, L., Mao, F., Yue, Q., Zhang, P., Jing, S., et al. (2017). ACBD 3 functions as a scaffold to organize the Golgi stacking proteins and a Rab33b- GAP. FEBS Lett. *591*, 2793–2802. https://doi.org/10.1002/1873-3468.12780.
33. Grant, B., and Hirsh, D. (1999). Receptor-mediated Endocytosis in the Caenorhabditis elegans Oocyte. Mol. Biol. Cell *10*, 4311–4326. https://doi.org/10.1091/mbc.10.12.4311.
34. Zhou, Y., Wang, X., Song, M., He, Z., Cui, G., Peng, G., Dieterich, C., Antebi, A., Jing, N., and Shen, Y. (2019). A secreted microRNA disrupts autophagy in distinct tissues of Caenorhabditis elegans upon ageing. Nat. Commun. *10*, 4827. https://doi.org/10.1038/s41467-019-12821-2.
35. Pan, X., Eathiraj, S., Munson, M., and Lambright, D.G. (2006). TBC-domain GAPs for Rab GTPases accelerate GTP hydrolysis by a dual-finger mechanism. Nature *442*, 303–306. https://doi.org/10.1038/nature04847.
36. Duan, X., Xu, L., Li, Y., Jia, L., Liu, W., Shao, W., Bayat, V., Shang, W., Wang, L., Liu, J.-P., and Tong, C. (2021). Regulation of lipid homeostasis by the TBC protein dTBC1D22 via modulation of the small GTPase Rab40 to facilitate lipophagy. Cell Rep. *36*, 109541. https://doi.org/10.1016/j.celrep.2021.109541.
37. Kim, W., Underwood, R.S., Greenwald, I., and Shaye, D.D. (2018). OrthoList 2: A New Comparative Genomic Analysis of Human and Caenorhabditis elegans Genes. Genetics *210*, 445–461. https://doi.org/10.1534/genetics.118.301307.
38. Mangahas, P.M., Yu, X., Miller, K.G., and Zhou, Z. (2008). The small GTPase Rab2 functions in the removal of apoptotic cells in Caenorhabditis elegans. J. Cell Biol. *180*, 357–373. https://doi.org/10.1083/jcb.200708130.
39. Yin, J., Huang, Y., Guo, P., Hu, S., Yoshina, S., Xuan, N., Gan, Q., Mitani, S., Yang, C., and Wang, X. (2017). GOP-1 promotes apoptotic cell degradation by activating the small GTPase Rab2 in C. elegans. J. Cell Biol. *216*, 1775–1794. https://doi.org/10.1083/jcb.201610001.
40. Sumakovic, M., Hegermann, J., Luo, L., Husson, S.J., Schwarze, K., Olendrowitz, C., Schoofs, L., Richmond, J., and Eimer, S. (2009). UNC-108/RAB-2 and its effector RIC-19 are involved in dense core vesicle maturation in Caenorhabditis elegans. J. Cell Biol. *186*, 897–914. https://doi.org/10.1083/jcb.200902096.
41. Ailion, M., Hannemann, M., Dalton, S., Pappas, A., Watanabe, S., Hegermann, J., Liu, Q., Han, H.-F., Gu, M., Goulding, M.Q., et al. (2014). Two Rab2 Interactors Regulate Dense-Core Vesicle Maturation. Neuron *82*, 167–180. https://doi.org/10.1016/j.neuron.2014.02.017.
42. Sato, K., Norris, A., Sato, M., and Grant, B.D. (2014). C. elegans as a model for membrane traffic. WormBook, 1–47. https://doi.org/10.1895/wormbook.1.77.2.
43. Elias, M., Brighouse, A., Gabernet-Castello, C., Field, M.C., and Dacks, J.B. (2012). Sculpting the endomembrane system in deep time: high resolution phylogenetics of Rab GTPases. J. Cell Sci. *125*, 2500–2508. https://doi.org/10.1242/jcs.101378.
44. Guo, P., Hu, T., Zhang, J., Jiang, S., and Wang, X. (2010). Sequential action of Caenorhabditis elegans Rab GTPases regulates phagolysosome formation during apoptotic cell degradation. Proc. Natl. Acad. Sci. USA *107*, 18016–18021. https://doi.org/10.1073/pnas.1008946107.
45. Harterink, M., Port, F., Lorenowicz, M.J., McGough, I.J., Silhankova, M., Betist, M.C., van Weering, J.R.T., van Heesbeen, R.G.H.P., Middelkoop, T.C., Basler, K., et al. (2011). A SNX3-dependent retromer pathway mediates retrograde transport of the Wnt sorting receptor Wntless and is required for Wnt secretion. Nat. Cell Biol. *13*, 914–923. https://doi.org/10.1038/ncb2281.
46. McGough, I.J., de Groot, R.E.A., Jellett, A.P., Betist, M.C., Varandas, K.C., Danson, C.M., Heesom, K.J., Korswagen, H.C., and Cullen, P.J. (2018). SNX3-retromer requires an evolutionary conserved MON2:DOPEY2:ATP9A complex to mediate Wntless sorting and Wnt secretion. Nat. Commun. *9*, 3737. https://doi.org/10.1038/s41467-018-06114-3.
47. Jung, Y., Artan, M., Kim, N., Yeom, J., Hwang, A.B., Jeong, D.-E., Altintas, Ö., Seo, K., Seo, M., Lee, D., et al. (2021). MON-2, a Golgi protein, mediates autophagy-dependent longevity in *Caenorhabditis elegans*. Sci. Adv. *7*, eabj8156. https://doi.org/10.1126/sciadv.abj8156.
48. Valadi, H., Ekström, K., Bossios, A., Sjöstrand, M., Lee, J.J., and Lötvall, J.O. (2007). Exosome-mediated transfer of mRNAs and microRNAs is a novel mechanism of genetic exchange between cells. Nat. Cell Biol. *9*, 654–659. https://doi.org/10.1038/ncb1596.
49. Zhao, Y., Holmgren, B.T., and Hinas, A. (2017). The conserved SNARE SEC-22 localizes to late endosomes and negatively regulates RNA interference in *Caenorhabditis elegans*. RNA *23*, 297–307. https://doi.org/10.1261/rna.058438.116.
50. Zhang, P., Wu, Y., Belenkaya, T.Y., and Lin, X. (2011). SNX3 controls Wingless/Wnt secretion through regulating retromer-dependent recycling of Wntless. Cell Res. *21*, 1677–1690. https://doi.org/10.1038/cr.2011.167.
51. Lorenowicz, M.J., Macurkova, M., Harterink, M., Middelkoop, T.C., de Groot, R., Betist, M.C., and Korswagen, H.C. (2014). Inhibition of late endosomal maturation restores Wnt secretion in Caenorhabditis elegans vps-29 retromer mutants. Cell. Signal. *26*, 19–31. https://doi.org/10.1016/j.cellsig.2013.09.013.
52. Gao, J., Zhao, L., Luo, Q., Liu, S., Lin, Z., Wang, P., Fu, X., Chen, J., Zhang, H., Lin, L., and Shi, A. (2020). An EHBP-1-SID-3-DYN-1 axis promotes membranous tubule fission during endocytic recycling. PLoS Genet. *16*, e1008763. https://doi.org/10.1371/journal.pgen.1008763.
53. Kaletsky, R., Moore, R.S., Vrla, G.D., Parsons, L.R., Gitai, Z., and Murphy, C.T. (2020). C. elegans interprets bacterial non-coding RNAs to learn pathogenic avoidance. Nature *586*, 445–451. https://doi.org/10.1038/s41586-020-2699-5.
54. Brenner, S. (1974). The Genetics of CAENORHABDITIS ELEGANS. Genetics *77*, 71–94.
55. Suehiro, Y., Yoshina, S., Motohashi, T., Iwata, S., Dejima, K., and Mitani, S. (2021). Efficient collection of a large number of mutations by mutagenesis of DNA damage response defective animals. Sci. Rep. *11*, 7630. https://doi.org/10.1038/s41598-021-87226-7.
56. Zuryn, S., Le Gras, S., Jamet, K., and Jarriault, S. (2010). A Strategy for Direct Mapping and Identification of Mutations by Whole-Genome Sequencing. Genetics *186*, 427–430. https://doi.org/10.1534/genetics.110.119230.
57. Friedland, A.E., Tzur, Y.B., Esvelt, K.M., Colaiácovo, M.P., Church, G.M., and Calarco, J.A. (2013). Heritable genome editing in C. elegans via a CRISPR-Cas9 system. Nat. Methods *10*, 741–743. https://doi.org/10.1038/nmeth.2532.
58. Dickinson, D.J., Ward, J.D., Reiner, D.J., and Goldstein, B. (2013). Engineering the Caenorhabditis elegans genome using Cas9-triggered homologous recombination. Nat. Methods *10*, 1028–1034. https://doi.org/10.1038/nmeth.2641.
59. Dejima, K., Hori, S., Iwata, S., Suehiro, Y., Yoshina, S., Motohashi, T., and Mitani, S. (2018). An Aneuploidy-Free and Structurally Defined Balancer Chromosome Toolkit for Caenorhabditis elegans. Cell Rep. *22*, 232–241. https://doi.org/10.1016/j.celrep.2017.12.024.
60. Schindelin, J., Arganda-Carreras, I., Frise, E., Kaynig, V., Longair, M., Pietzsch, T., Preibisch, S., Rueden, C., Saalfeld, S., Schmid, B., et al. (2012). Fiji: an open-source platform for biological-image analysis. Nat. Methods *9*, 676–682. https://doi.org/10.1038/nmeth.2019.
61. Kanda, Y. (2013). Investigation of the freely available easy-to-use software 'EZR' for medical statistics. Bone Marrow Transplant. *48*, 452–458. https://doi.org/10.1038/bmt.2012.244.

STAR★METHODS

KEY RESOURCES TABLE

REAGENT or RESOURCE	SOURCE	IDENTIFIER
Bacterial and virus strains		
OP50-1	Chalfie lab	N/A
HT115	Caenorhabditis Genetics Center (CGC)	N/A
Chemicals, peptides, and recombinant proteins		
isopropyl β-D-1-thiogalactopyranoside (IPTG)	Sigma Aldrich	I6758
Deposited data		
Whole genome sequence data (tm9739)	This study	NCBI Trace Archive: SRR24389897
Whole genome sequence data (tm9742)	This study	NCBI Trace Archive: SRR24389896
Whole genome sequence data (tm9743)	This study	NCBI Trace Archive: SRR24389895
Whole genome sequence data (tm9739_x5)	This study	NCBI Trace Archive: SRR24389894
Whole genome sequence data (tm9742_x5)	This study	NCBI Trace Archive: SRR24389893
Whole genome sequence data (tm9743_x5)	This study	NCBI Trace Archive: SRR24389892
Whole genome sequence data (tm9833;tm9924)	This study	NCBI Trace Archive: SRR24389891
Experimental models: Organisms/strains		
C. elegans wild type	CGC	N2
C. elegans: Strain: FX13285: *aex-6(tm2302) I; rab-3(tm3275) II*	This study	FX13285
C. elegans: Strain: FX30943: *rab-3(tm3275) II; rexd-1(tm9739) III*	This study	FX30943
C. elegans: Strain: FX30945: *rexd-1(tm9743) III*	This study	FX30945
C. elegans: Strain: FX31895: *rexd-1(tm11388) III*	NBRP	FX31895
C. elegans: Strain: FX31896: *aex-6(tm2302) I; rab-3(tm3275) II; rexd-1(tm11388) III*	This study	FX31896
C. elegans: Strain: FX31272: *rexd-1(tm11388) III; tmEx5176[vha-6p::rexd-1a::TagRFP; myo-2p::venus]*	This study	FX31272
C. elegans: Strain: FX31279: *rexd-1(tm11388) III; tmEx5191[dpy-7p::rexd-1a::TagRFP; myo-2p::venus]*	This study	FX31279
C. elegans: Strain: FX31275: *rexd-1(tm11388) III; tmEx5179[vha-6p::rexd-1b::TagRFP; myo-2p::venus]*	This study	FX31275
C. elegans: Strain: FX31282: *rexd-1(tm11388) III; tmEx5194[dpy-7p::rexd-1b::TagRFP; myo-2p::venus]*	This study	FX31282
C. elegans: Strain: FX31286: *rexd-1(tm11388) III; pwIs170[Pvha6::GFP::rab-7 + Cbr-unc-119(+)]; tmEx5176[vha-6p::rexd-1a::TagRFP; myo-2p::venus]*	This study and CGC	FX31286
C. elegans: Strain: FX31856: *rexd-1(tm11388) III; pwIs50[Plmp-1::lmp-1::GFP + Cbr-unc-119(+)]; tmEx5176[vha-6p::rexd-1a::TagRFP; myo-2p::venus]*	This study and CGC	FX31856
C. elegans: Strain: FX31288: *rexd-1(tm11388) III; pwIs72[vha-6p::GFP::rab-5 + Cbr-unc-119(+)] II; tmEx5176[vha-6p::rexd-1a::TagRFP; myo-2p::venus]*	This study and CGC	FX31288
C. elegans: Strain: FX31287: *rexd-1(tm11388) III; pwIs69[vha6p::GFP::rab-11 + unc-119(+)] X; tmEx5176 [vha-6p::rexd-1a::TagRFP; myo-2p::venus]*	This study and CGC	FX31287

(*Continued on next page*)

Continued

REAGENT or RESOURCE	SOURCE	IDENTIFIER
C. elegans: Strain: FX31289: *rexd-1(tm11388) III; pwIs503[vha-6p::mans::GFP + Cbr-unc-119(+)]; tmEx5176[vha-6p::rexd-1a::TagRFP; myo-2p::venus]*	This study and CGC	FX31289
C. elegans: Strain: FX31857: *pwIs170[Pvha6::GFP::rab-7 + Cbr-unc-119(+)]; tmEx5179[vha-6p::rexd-1b::TagRFP; myo-2p::venus]*	This study and CGC	FX31857
C. elegans: Strain: FX31858: *pwIs50[Plmp-1::lmp-1::GFP + Cbr-unc-119(+)]; tmEx5179[vha-6p::rexd-1b::TagRFP; myo-2p::venus]*	This study and CGC	FX31858
C. elegans: Strain: FX31290: *rexd-1(tm11388) III; tmEx5281[dpy-7p::rexd-1a::TagRFP; dpy-7p::venus::rab-7]*	This study	FX31290
C. elegans: Strain: FX31859: *rexd-1(tm11388) III; tmEx5300[dpy-7p::rexd-1a::TagRFP; col-19p::lmp-1::venus]*	This study	FX31859
C. elegans: Strain: FX31296: *rexd-1(tm11388) III; tmEx5289[dpy-7p::rexd-1a::TagRFP; dpy-7p::venus::rab-5]*	This study	FX31296
C. elegans: Strain: FX31292: *rexd-1(tm11388) III; tmEx5283[dpy-7p::rexd-1a::TagRFP; dpy-7p::venus::rab-11]*	This study	FX31292
C. elegans: Strain: FX31294: *rexd-1(tm11388) III; tmEx5285[dpy-7p::rexd-1a::TagRFP; dpy-7p::aman-2::venus]*	This study	FX31294
C. elegans: Strain: FX31860: *tmEx5163[rexd-1p::GFP; myo-2p::mCherry]*	This study	FX31860
C. elegans: Strain: FX30944: *tbc-3(tm9742) rde-11(tm9860) IV*	This study	FX30944
C. elegans: Strain: FX31065: *tbc-3(tm9742) rde-11(tm9860) IV; tmEx5091[rde-11(+); myo-2p::mCherry]*	This study	FX31065
C. elegans: Strain: FX31067: *tbc-3(tm9742) rde-11(tm9860) IV; tmEx5107[tbc-3(+); rde-11(+); myo-2p::mCherry]*	This study	FX31067
C. elegans: Strain: FX9833: *tbc-3(tm9833) IV*	This study	FX9833
C. elegans: Strain: FX31861: *tbc-3(tm9833) IV; tmEx5404[vha-6p::TagRFP::tbc-3a; myo-2p::venus]*	This study	FX31861
C. elegans: Strain: FX31862: *tbc-3(tm9833) IV; tmEx5406[vha-6p::TagRFP::tbc-3b; myo-2p::venus]*	This study	FX31862
C. elegans: Strain: FX31863: *tbc-3(tm9833) IV; tmEx5414[dpy-7p::TagRFP::tbc-3a; myo-2p::venus]*	This study	FX31863
C. elegans: Strain: FX31864: *tbc-3(tm9833) IV; tmEx5415[dpy-7p::TagRFP::tbc-3b; myo-2p::venus]*	This study	FX31864
C. elegans: Strain: FX31865: *tbc-3(tm9833) IV; pwIs503 [vha-6p::mans::GFP + Cbr-unc-119(+)]; tmEx5405[vha-6p::TagRFP::tbc-3b; myo-2p::venus]*	This study and CGC	FX31865
C. elegans: Strain: FX31866: *tbc-3(tm9833) IV; pwIs170 [Pvha6::GFP::rab-7 + Cbr-unc-119(+)]; tmEx5405[vha-6p::TagRFP::tbc-3b; myo-2p::venus]*	This study and CGC	FX31866
C. elegans: Strain: FX19502: *sid-5(tm4328) X*	NBRP	FX19502

(*Continued on next page*)

Continued

REAGENT or RESOURCE	SOURCE	IDENTIFIER
C. elegans: Strain: FX31867: *rexd-1(tm11388) III; tbc-3(tm9833) IV*	This study	FX31867
C. elegans: Strain: FX31868: *rexd-1(tm11388) III; sid-5(tm4328) X*	This study	FX31868
C. elegans: Strain: FX31869: *tbc-3(tm9833) IV; sid-5(tm4328) X*	This study	FX31869
C. elegans: Strain: FX31870: *rexd-1(tm11388) III; tbc-3(tm9833) IV; sid-5(tm4328) X*	This study	FX31870
C. elegans: Strain: FX09006: *rsd-3(tm9006) X*	Imae et al.[17]	FX09006
C. elegans: Strain: NL2507: *pkIs1582[let-858::GFP + rol-6(su1006)]*	CGC	NL2507
C. elegans: Strain: FX31871: *rexd-1(tm11388) III; tbc-3(tm9833) IV; sid-5(tm4328) X; pkIs1582[let-858::GFP + rol-6(su1006)]*	This study and CGC	FX31871
C. elegans: Strain: FX31872: *pkIs1582[let-858::GFP + rol-6(su1006)]; tmIs1059[snb-1p::gfp_hairpin; myo-2p::mCherry]*	This study and CGC	FX31872
C. elegans: Strain: FX31873: *rexd-1(tm11388) III; tbc-3(tm9833) IV; sid-5(tm4328) X; pkIs1582[let-858::GFP + rol-6(su1006)]; tmIs1059[snb-1p::gfp_hairpin; myo-2p::mCherry]*	This study and CGC	FX31873
C. elegans: Strain: FX14985: *rsd-3(tm9006) X; pkIs1582 [let-858::GFP + rol-6(su1006)]*	Imae et al.[17]	FX14985
C. elegans: Strain: FX02700: *sid-1(tm2700) V*	NBRP	FX02700
C. elegans: Strain: FX31874: *rexd-1(tm11388) III; tbc-3(tm9833) IV; sid-5(tm4328) X; tmEx5176[vha-6p::rexd-1a::TagRFP; myo-2p::venus]*	This study	FX31874
C. elegans: Strain: FX31875: *rexd-1(tm11388) III; tbc-3(tm9833) IV; sid-5(tm4328) X; tmEx5406[vha-6p::TagRFP::tbc-3b; myo-2p::venus]*	This study	FX31875
C. elegans: Strain: FX31876: *rexd-1(tm11388) III; tbc-3(tm9833) IV; sid-5(tm4328) X ;tmEx5689[vha-6p::sid-5; myo-2p::mCherry]*	This study	FX31876
C. elegans: Strain: FX18346: *bIs1[Pvit-2::VIT-2::GFP; rol-6(su1006)]*, derived from DH1033	CGC	FX18346
C. elegans: Strain: FX31877: *rexd-1(tm11388) III; tbc-3(tm9833) IV; sid-5(tm4328) X; bIs1[Pvit-2::VIT-2::GFP; rol-6(su1006)]*	This study and CGC	FX31877
C. elegans: Strain: RT258: *pwIs50[Plmp-1::lmp-1::GFP + Cbr-unc-119(+)]*	CGC	RT258
C. elegans: Strain: FX31878: *rexd-1(tm11388) III; tbc-3(tm9833) IV; sid-5(tm4328) X; pwIs50[Plmp-1::lmp-1::GFP + Cbr-unc-119(+)]*	This study and CGC	FX31878
C. elegans: Strain: FX31879: *tbc-3(tm9833) IV; tmEx5562[dpy-7p::TagRFP::tbc-3bRQ-AA; myo-2p::venus]*	This study	FX31879
C. elegans: Strain: FX31880: *rab-33(tm2641) III; tbc-3(tm9833) IV*	This study and NBRP	FX31880
C. elegans: Strain: FX31881: *tbc-3(tm9833) IV; rabr-1(tm2564) X*	This study and NBRP	FX31881

(*Continued on next page*)

Continued

REAGENT or RESOURCE	SOURCE	IDENTIFIER
C. elegans: Strain: FX31882: *unc-108(tm9924) I; tbc-3(tm9833) IV*	This study	FX31882
C. elegans: Strain: FX31883: *unc-108(tm9924) I; tbc-3(tm9833) IV; tmEx5716[unc-108(+); myo-2p::venus]*	This study	FX31883
C. elegans: Strain: ZH382: *unc-108(n3263) I*	CGC	ZH382
C. elegans: Strain: FX31884: *unc-108(n3263) I; tbc-3(tm9833) IV*	This study	FX31884
C. elegans: Strain: FX05384: *gop-1(tm5384) III*	NBRP	FX05384
C. elegans: Strain: FX31885: *gop-1(tm5384) III; tbc-3(tm9833) IV*	This study	FX31885
C. elegans: Strain: FX02095: *rab-14(tm2095) X*	NBRP	FX02095
C. elegans: Strain: FX9826: *rabr-4 rabr-3(tm9826) V*	This study	FX9826
C. elegans: Strain: RB946: *ric-19(ok833) I*	CGC	RB946
C. elegans: Strain: EG334: *cccp-1(ox334) III*	CGC	EG334
C. elegans: Strain: FX03622: *rund-1(tm3622) X*	NBRP	FX03622
C. elegans: Strain: FX01595: *snx-3(tm1595) I*	NBRP	FX01595
C. elegans: Strain: FX02605: *mon-2(tm2605) IV*	NBRP	FX02605
C. elegans: Strain: FX31886: *snx-3(tm1595)/tmC18 [dpy-5(tmIs1200)] I; mon-2(tm2605) IV*	This study and NBRP	FX31886
C. elegans: Strain: FX31887: *snx-3(tm1595) I; tbc-3(tm9833) IV*	This study	FX31887
C. elegans: Strain: FX31888: *tbc-3(tm9920) mon-2(tm2605) IV*	This study	FX31888
C. elegans: Strain: FX31889: *snx-3(tm1595) I; sid-5(tm4328) X*	This study	FX31889
C. elegans: Strain: FX31890: *mon-2(tm2605) IV; sid-5(tm4328) X*	This study	FX31890
C. elegans: Strain: FX31891: *snx-3(tm1595) I; rexd-1(tm11388) III*	This study	FX31891
C. elegans: Strain: FX31892: *rexd-1(tm11388) III; mon-2(tm2605) IV*	This study	FX31892
C. elegans: Strain: FX31893: *rab-18(tm2121) III; tbc-3(tm9833) IV*	This study and NBRP	FX31893
C. elegans: Strain: FX31894: *tbc-3(tm9833) IV; glo-1(tm3240) X*	This study and NBRP	FX31894
Recombinant DNA		
plasmid for *tbc-3* CRISPR	This study	NA
plasmid for *rabr-4&rabr-3* CRISPR	This study	NA
Pmyo-2::mCherry	Addgene	pCFJ90, Addgene Plasmid #19327
myo-2p::Venus	Dejima et al.[59]	pFX_Pmyo-2::Venus
vha-6p::rexd-1a::TagRFP	This study	NA
vha-6p::rexd-1b::TagRFP	This study	NA
dpy-7p::rexd-1a::TagRFP	This study	NA
dpy-7p::rexd-1a::TagRFP	This study	NA
rexd-1p::GFP	This study	NA
vha-6p:: TagRFP::tbc-3a	This study	NA
vha-6p:: TagRFP::tbc-3b	This study	NA

(*Continued on next page*)

Continued

REAGENT or RESOURCE	SOURCE	IDENTIFIER
dpy-7p:: TagRFP::tbc-3a	This study	NA
dpy-7p:: TagRFP::tbc-3b	This study	NA
vha-6p::sid-5	This study	NA
dpy-7p:: TagRFP::tbc-3bRQ-AA	This study	NA
Software and algorithms		
Fiji	Schindelin et al.[60]	RRID:SCR_002285
EZR	Kanda[61]	https://www.jichi.ac.jp/saitama-sct/SaitamaHP.files/statmedEN.html

RESOURCE AVAILABILITY

Lead contact

Further information and requests for resources and reagents should be directed to and will be fulfilled by the lead contact, Shohei Mitani (mitani.shohei@twmu.ac.jp).

Materials availability

New strains and reagents generated in this study are available through the lead contact.

Data and code availability

The whole-genome sequencing data generated in this study have been submitted to the NCBI BioProject database under accession number PRJNA964498. Accession numbers are NCBI Trace Archive: SRR24389897, NCBI Trace Archive: SRR24389896, NCBI Trace Archive: SRR24389895, NCBI Trace Archive: SRR24389894, NCBI Trace Archive: SRR24389893, NCBI Trace Archive: SRR24389892 and NCBI Trace Archive: SRR24389891. Data reported in this paper will be shared by the lead contact upon request.
This paper does not report original code.
Any additional information required to reanalyze the data reported in this paper is available from the lead contact upon request. Source data are provided with this paper.

EXPERIMENTAL MODEL AND STUDY PARTICIPANT DETAILS

Bristol N2 was used as wild type strain. Culture conditions, genetic crosses, and other *C. elegans* methods were performed according to standard protocols[54] except where otherwise indicated. All experiments were performed at 20°C. Detailed information on the strains used in this study is included in the key resources table.

METHOD DETAILS

Forward genetic screens

For identification of mutants defective in feeding RNAi, approximately 10,000 young adult staged *aex-6(tm2302); rab-3(tm3275)* animals were mutagenized in 50 mM EMS for 4 h. F3 animals were subjected to *bli-3* feeding RNAi, which causes larval lethality in an RNAi-sensitive background. To circumvent isolating mutants for previously defined RNAi defective (Rde) genes, animals that show strong resistance to RNAi (without phenotype) were excluded, and weak resistant animals, with blisters but viable, were screened for further analysis. Resultant strains were then sequenced (1st round WGS) to exclude strains that had homozygous mutations in Rde genes such as *rde*, *sid* and *rsd*. Candidate strains were outcrossed with N2 five times and subsequently sequenced to map and identify causal mutations (2nd round WGS). Note that the *rde-10(tm9860)* mutation was identified as heterozygous in the 1st round of WGS but was detected as homozygous in the 2nd round of sequencing.

To screen the *tbc-3* suppressor, 4,000 P0 *tbc-3(tm9833)* animals were mutagenized. F3 progenies were screened for increased sensitivity to *bli-1* feeding RNAi. Candidate strains were sequenced after backcrossing to the original unmutagenized strain five times.

Whole-genome sequencing and mutation mapping

Genomic DNA was isolated using a DNeasy Blood & Tissue Kit (Qiagen). A DNA library was prepared from genomic DNA with a LibraryBuilder automatic library synthesis machine (Thermo Fisher Scientific) as described previously.[55] The DNA library was used for the construction of templates by the ionChef system (Thermo Fisher Scientific), and the templates were sequenced to a target depth of approximately 20-25 (1st round WGS) or a target depth of approximately 35-40 (2nd round WGS) using ionProton (Thermo Fisher Scientific) according to the standard protocol. Small variants were identified with variantCaller (https://github.com/iontorrent/TS/tree/master/plugin/variantCaller) or

GoogleDeepVariant (https://github.com/google/deepvariant). The genomic region linked to the causal mutation of each strain was determined by mapping unique EMS-induced variants in the outcrossed strain,[56] and change-of-function mutations in this region were identified as candidates.

CRISPR/Cas9-mediated genome editing

For generation of deletion mutants for the *tbc-3*, *rabr-4* and *rabr-3* genes, we used the plasmid-based CRISPR/Cas9 method.[57,58] We constructed multiguide Cas9/sgRNA plasmids containing two U6 promoter::sgRNAs[59] using a Clontech In-Fusion PCR Cloning Kit (Clontech Laboratories, Palo Alto, CA). We injected a multiguide Cas9/sgRNA plasmid (50 ng/μl), the injection marker plasmid pCFJ90 (Pmyo-2::mCherry, a gift from Erik Jorgensen; Addgene plasmid # 19327) (5 ng/μl) and pBluescript KS(+)T1 (pBKS) (145 ng/μl) into the gonads of wild-type or *mon-2*(*tm2605*) animals. Deletions were identified by PCR screening and confirmed by Sanger sequencing. Deletion regions of each allele are as follows: *tbc-3(tm9833)*: [F32B6]20889/20890-22500/22501 (1611 bp deletion), *tbc-3(tm9920)*: [F32B6]20932/20933-22467/22468 (1535 bp deletion), *rabr-4&rabr-3 (tm9826)*: [F11A5]4750/4751-GGAAA-6745/6746 (1995 bp deletion + 5 bp insertion).

Generation of transgenic animals

For *rexd-1* rescue experiments, plasmid constructs consisting of the *vha-6* or *dpy-7* promoter region and *rexd-1a* or *rexd-1b* cDNA fused with TagRFP were generated and individually injected (20 ng/μl) with a *myo-2p::Venus* (5 ng/μl) injection marker and pBKS (175 ng/μl) into *rexd-1(tm11388)*, and the resultant lines, *tmEx5176*, *tmEx5179*, *tmEx5191* and *tmEx5194*, were analyzed. To observe the subcellular localization of REXD-1 in the hypodermis, the *dpy-7p::rexd-1::TagRFP* construct (20 ng/μl) and each organelle marker construct (20 ng/μl) were injected with pBKS (160 ng/μl) into *rexd-1(tm11388)*. To generate the *rexd-1* transcription reporter, the 5′ flanking region of *Y39A3CL.7* (926 bp + 37 bp CDS), which is the 5′ adjacent gene to *Y39A3CL.1* in an operon (CEOP3068: WormBase), was isolated as a putative *rexd-1* promoter and inserted into pPD95.75 (a gift from Dr. A. Fire). The resultant plasmid (*rexd-1p::GFP*) was injected (50 ng/μl) with pCFJ90 (5 ng/μl) and pBKS (145 ng/μl) into the wild type. For the FX30944 rescue experiment, the *rde-11* locus, from 667 upstream to 27 bp downstream of the coding region, and the *tbc-3* locus, from 2694 bp upstream to 65 bp downstream of the coding region, were amplified by PCR. To generate *tmEx5091*, a PCR fragment of *rde-11* was injected (20 ng/μl) with pCFJ90 (5 ng/μl) and pBKS (175 ng/μl) into FX30944. To generate *tmEx5107*, PCR fragments of *rde-11* (20 ng/μl) and *tbc-3* (30 ng/μl) were injected with pCFJ90 (5 ng/μl) and pBKS (145 ng/μl) into FX30944. For *tbc-3* rescue experiments, plasmid constructs consisting of the *vha-6* or *dpy-7* promoter region and *tbc-3a* or *tbc-3b* cDNA fused with TagRFP were generated and individually injected (20 ng/μl) with *myo-2p::Venus* (5 ng/μl) and pBKS (175 ng/μl) into *tbc-3(tm9833)*, and the resultant lines, *tmEx5404*, *tmEx5406*, *tmEx5414* and *tmEx5415*, were analyzed. To generate *tmIs1059*, an extrachromosomal array containing *snb-1p::gfp_hairpin* and *myo-2p::DsRedm* was integrated using UV irradiation and outcrossed with the wild type. To generate *tmEx5689*, *vha-6p::sid-5* (1 ng/μl), pCFJ90 (5 ng/μl) and pBKS (194 ng/μl) were injected into *rexd-1(tm11388); tbc-3(tm9833); sid-5(tm4328)*. To generate *tmEx5562*, *dpy-7p::TagRFP::tbc-3bRQ-AA* was constructed by introducing point mutations into wild-type *tbc-3b* to substitute arginine257 and glutamine292 with alanine residues and injected (20 ng/μl) with *myo-2p::Venus* (5 ng/μl) and pBKS (175 ng/μl) into *tbc-3(tm9833)*. For the *unc-108* rescue experiment, the *unc-108* locus, from 816 upstream to 498 bp downstream of the coding region, was amplified by PCR, and the PCR fragment was injected (10 ng/μl) with pCFJ90 (5 ng/μl) and pBKS (185 ng/μl) into the suppressor strain carrying the *unc-108(tm9924)* mutation.

RNAi experiments

Feeding RNAi was performed as described previously.[6] RNAi clones were transformed into E. coli HT115(DE3), and the bacteria were grown on NGM supplemented with 100 μg/mL ampicillin and 1 mM isopropyl-beta-D-thiogalactopyranoside (IPTG). RNAi clones were obtained from the Ahringer library (GeneService), except for clones for *rab-19*, *rab-27*, *rab-30* and *C56E6.2*, which were obtained from the Vidal library (Open Biosystems). RNAi clones for GFP were constructed previously.[17] For the *bli-1*, *bli-3*, *act-5*, *elt-2* and *lin-1* RNAi assays, L1 larvae were fed bacteria possessing each of the RNAi clones, and 48 h later, animals showing partial or whole-body blisters, larval lethality or blisters, larval arrest, clear, and multivulva or protruding vulva phenotypes were scored. For *unc-15* RNAi, L1 larvae were placed on RNAi plates, and 72 h later, the percentage of animals showing Unc (paralysis) was scored. For the *pos-1* feeding RNAi assay, animals were cultured on RNAi plates from the L1 to Day 2 adult stages. Ten adult animals were transferred to new NGM plates, allowed to lay eggs for several hours and then removed. Twenty-four hours later, the percentage of dead eggs was scored. For lower-dose (desensitized) conditions, bacteria expressing *pos-1* dsRNA were diluted in the indicated ratio with LB medium before seeding on NGM plates. For GFP feeding RNAi, animals were cultured on RNAi plates from the L1 to L4 stages, and animals with repressed intestinal GFP expression were scored. For the RNAi experiment by microinjection, synthesized *pos-1* dsRNA was prepared at a concentration of 10 ng/μl as described previously[17] and injected into the pseudocoelom of Day 1 adult hermaphrodites. The lethality of embryos laid between 12 to 24 hours post injection was scored for each injected animal. For RNAi screening for the *tbc-3* suppressor, Day 1 adult *tbc-3(tm9833)* animals were placed on plates seeded with bacteria expressing dsRNA targeting each of the *rab* genes or GFP control and allowed to lay eggs for several hours. L1 staged F1 progenies were then transferred to RNAi plates seeded with a 1:1 mixture of *rab* clones and *bli-1* dsRNA clones, and 48 h later, the sensitivity to *bli-1* RNAi was compared between control and *rab* knockdown animals.

Microscopy

Animals were immobilized with M9 buffer containing 50 mM sodium azide on a 5% agarose pad containing 10 mM sodium azide. Fluorescence images were obtained using a BX51 microscope equipped with a DP80 CCD camera (Olympus Optical). Confocal microscopic images were captured using LSM710 or LSM510 (Carl Zeiss). For measurement of the diameter of LMP-1::GFP-positive vesicles, pictures of coelomocytes in animals carrying the *pwIs50* transgene were captured, and the diameter of the largest LMP-1::GFP in each coelomocyte was measured using FIJI.[60] Worms on NGM plates were imaged with DP30BW CCD camera (Olympus Optical) using DPController imaging software.

QUANTIFICATION AND STATISTICAL ANALYSIS

The standard error of the mean (SEM) was used as the error bar for bar graphs plotted from the mean value of the data from three independent experiments, unless otherwise indicated. Statistical analyses were performed using EZR.[61] Differences between two or multiple groups were compared using two-tailed Student's *t*-test or one-way ANOVA followed by Tukey's post hoc test, respectively. Data were considered significantly different if *P*-values were lower than 0.05.